AN ABSTRACT OF THE THESIS OF

Joseph L. Pikul Jr. for the degree of Master of Science in Soil Science presented on February 22, 1983

Title: Calculated and Field-Measured Soil Heat Flux: A Comparison Under Two Soil Water Regimes

Abstract approved: Redacted for Privacy
Raymond R. Allmaras

Heat and water vapor flow in summer-fallowed fields in the Pacific Northwest may significantly affect the position and supply of water for germination of fall sown crops. New tillage tools and drill openers used in reduced tillage systems leave a trashy, residue covered surface in contrast to the traditional bare fallow systems. It is likely that these new management techniques cause changes in heat and water flow that produce unique profiles of soil temperature and water content. There is a need to elucidate heat and mass flow theory under field conditions appropriate to these new tillage systems. However, heat and mass flow theory has been studied almost exclusively in the laboratory using uniformly packed homogeneous soil. Heat flow theory in these experiments has generally consisted of two components: de Vries theoretical estimation of soil thermal conductivity and the Philip formulation of total heat flux consisting of heat flow responses to thermal and moisture gradients.

The Philip-de Vries theory was field tested to determine if such theory could be used to project the water conservation aspects of reduced tillage systems. Soil heat flux was calculated using the

theory of Philip-de Vries and then compared with soil heat fluxes experimentally determined in a Walla Walla silt loam using a null-alignment of soil temperatures and calorimetric heat flow. Comparisons at 20 depths in the top 60 cm of soil were made during mid-summer on no-till field plots with two soil moisture regimes. All components of heat flow including vapor heat flux terms were used in the theoretical calculations, but isothermal vapor flux accounted for less than 1% of the total vapor flux.

Measured net daily heat flux at 0.25 cm was 22.3 and 21.7 cal cm^{-2} day^{-1} for the moist and dry treatments, respectively. Theoretical heat flux calculations at this same depth generally gave a tenfold overestimation of measured heat flux during those times of the day when large temperature gradients existed. At 9 cm, approximately the seeding depth of winter wheat, measured net daily heat flux was 14.5 and 20.6 cal cm^{-2} day^{-1} for the moist and dry treatments, respectively; respective theoretical fluxes were 15.7 and 32.8 cal cm^{-2} day^{-1}. Calculated total fluxes in the top 35 cm generally overestimated by 20 and 40 percent, as compared to measured fluxes, for the moist and dry treatments, respectively.

Theoretical heat flux vapor components were calculated as the difference between total and conduction heat fluxes. Soil water changes predicted by vapor flux theory agreed with measured seedzone diurnal water content changes on the dry plot. At 35 cm vapor fluxes were negligible. Heat flux by conduction at this same depth overestimated measured flux by 10% on both plots. At all depths theo-

retical heat flux by conduction was more seriously overestimated than the vapor components of heat flux.

The Philip-de Vries heat flux model satisfactorily predicted water changes in dry soil seedbeds by vapor flux theory. Overestimation of the conduction component of the de Vries thermal conductivity produced an overestimation of calculated heat flux on both plots at all depths. Further calibration of the conduction components of the model will be needed to continue assessment of heat and vapor flux in dry seedbeds.

Calculated and Field-Measured Soil Heat Flux: A Comparison Under Two Soil Water Regimes

by

Joseph L. Pikul Jr.

A THESIS

submitted to

Oregon State University

in partial fulfillment of
the requirements for the
degree of

Master of Science

Commencement June 1983

APPROVED:

Redacted for Privacy

Professor of Soil Science in charge of major

Redacted for Privacy

Head of Department of Soil Science

Redacted for Privacy

Dean of Graduate School

Date thesis is presented February 22, 1983

Typed by Carol Brehaut for Joseph L. Pikul Jr.

ACKNOWLEDGMENTS

I wish to express my appreciation to my thesis advisor, Dr. Raymond R. Allmaras for his personal involvement in my career development at the Agricultural Research Service, USDA, Pendleton, Or. In addition I am grateful for his valuable guidance and for the many hours of critical editing of this thesis.

I would like to thank USDA-ARS computer specialist Sue E. Waldman for the considerable task of writing the programs that made this research run smoothly.

Appreciation is also extended to the staff of the Agricultural Research Station at Pendleton for their support during this study. Special thanks are given to Mr. Gordon Fischbacher for his assistance in graphic presentation and Dr. Ronald W. Rickman for his helpful and timely discussions on the many aspects of this work.

Appreciation is expressed to Dr. Larry Boersma for his valuable guidance and advice during my stay at Oregon State University.

Finally, to my wife, Connie, I express deep appreciation for the encouragement and help she gave me during the course of this research effort.

TABLE OF CONTENTS

LIST OF FIGURES

LIST OF TABLES

LIST OF SYMBOLS

Major symbols used in the text are listed below.

Cl = calculated net isothermal liquid water flow into (or out of) a soil slab (cm).

Cw = measured net change in the water content of a soil slab (cm)

Da = diffusion coefficient for water vapor in air (cm^2/sec).

D,Do, and Ds= diffusion coefficients for an insoluble gas in moist soil, air, and dry soil, respectively (cm^2/sec).

$D\theta v$ = isothermal vapor diffusivity (cm^2/sec).

G = null alignment measured heat flux ($mcal/cm^2 \cdot sec$).

Gc = Philip-de Vries calculated heat flux ($mcal/cm^2 \cdot sec$).

G_r = 35-cm reference depth heat flux ($mcal/cm^2 \cdot sec$).

Go = conduction component of Gc ($mcal/cm^2 \cdot sec$).

Gv = vapor component of Gc ($mcal/cm^2 \cdot sec$).

H = volumetric heat capacity ($mcal/cm^3 \cdot C$).

K_a' = ratio of the space average of the temperature gradient in the soil air and the space average of the temperature gradient in dry air (dimensionless).

K_s' = ratio of the space average of the temperature gradient in the soil solids and the space average of the temperature gradient in dry air (dimensionless).

Ks,a = ratio of the space average of the temperature gradient in the soil solids(Ks) or air (Ka) and the space average of the temperature gradient in water (dimensionless).

$K(\theta)$ = hydraulic conductivity as a function of volumetric water content (cm/min).

L = latent heat of vaporization of water (mcal/g).

N = number of observations or distinct granules.

Or = organic matter (g/g).

P = total gas pressure (mbar).

Pv = partial vapor pressure of water (mbar).

R = gas constant (83144 mbar cm^3/mole·K).

T = temperature (°C).

V = volume of gas (cm^3).

Xa = volumetric fraction of gas filled pore.

Xm = volumetric fraction of mineral matter.

Xo = volumetric fraction of organic matter.

Xw = volumetric fraction of water.

Xs = volumetric fraction of solids.

a_o = average daily soil temperature as used in Fourier Series.

a_k = Kth harmonic coefficient as used in Fourier Series.

b_k = Kth harmonic coefficient as used in Fourier Series.

z = height above soil surface or depth below soil surface (cm).

q = isothermal liquid water flow (cm/min).

h = relative humidity of the soil air (fraction).

n = number of moles.

g_s = depolarization factor for solids = 0.144 (dimensionless).

g_a = depolarization factor for air (dimensionless).

v = water content change in a soil slab due to the net flux of water vapor (cm/day).

i = subscript for depth number or distinct soil component.

j = subscript for time counter.

λ = apparent thermal conductivity of the soil (mcal/cm·sec·C).

λc = conduction thermal conductivity (mcal/cm·sec·C).

λw = thermal conductivity of water (mcal/cm·sec·C).

λs = thermal conductivity of solids (9.98 mcal/cm·sec·C).

λa = thermal conductivity of dry air (mcal/cm·sec·C).

λv = vapor component of λav (mcal/cm·sec·C).

λav = apparent thermal conductivity of gas filled pore (mcal/cm·sec·C).

λr = thermal conductivity at the 35-cm reference depth (mcal/cm·sec·C).

λv^s = saturated vapor conductivity (mcal/cm·sec·C).

ρb = soil bulk density on dry weight basis (g/cm^3).

ρl = density of liquid water (g/cm^3).

ρo = saturated water vapor density (g/cm^3).

ρp = soil particle density (2.657 g/cm^3).

θ = volumetric water content (cm^3/cm^3).

θc = critical water content (cm^3/cm^3).

θg = gravimetric water content (g/g).

σ = geometry or tortuosity factor (dimensionless).

ε = total porosity fraction ($\varepsilon = 1 - \rho b/\rho p$).

εg = gas filled porosity fraction ($\varepsilon g = \varepsilon - \theta$).

ω = angular frequency as used in Fourier Series.

γ = mass flow factor (dimensionless).

$d\rho o/dT$ = saturated water vapor density gradient ($g/cm^3 \cdot C$).

dT/dt = derivative of temperature with respect to time (°C/min).

dT/dz = derivative of temperature with respect to depth, z (°C/cm).

$d\theta/dz$ = volumetric water content gradient (cm^{-1}).

dH/dz = hydraulic head gradient (cm/cm).

CALCULATED AND FIELD-MEASURED SOIL HEAT FLUX: A COMPARISON UNDER TWO SOIL WATER REGIMES

INTRODUCTION

Heat flow in bare and stubble covered soils is especially important because heat flow is usually large and is coupled with moisture flow. Soil temperature responses to soil heat flow during the warm part of the season alter the exchange of heat between the air and soil. They may also affect plant response in the seedbed of winter wheat. In the winter soil temperature responses may directly affect the freezing and thawing of soil which in turn may affect runoff and erosion. In an arid to semiarid agriculture such as in the Pacific Northwest, the coupled heat and moisture flow undoubtedly is a critical factor in the management of summerfallow and seedbeds for winter wheat. Magnitudes of these heat and moisture flow phenomena and their sensitivity to tillage and residue management would indeed be useful, but few field experiments have been conducted.

Summerfallow is practiced in the Pacific Northwest to retain, over the warm dry summer, water stored in the soil during the previous winter recharge (Leggett et al., 1974). Summerfallow in the Pacific Northwest is unique because it must maintain enough water at shallow depths to germinate winter wheat (Triticum aestivum L.) before the winter rainy season begins (Papendick et al., 1973; Leggett et al., 1974). Maintenance of soil moisture at a depth less than 20 cm during the warm dry summer and early fall requires special tillage management. Small grain stubble is usually moldboard plowed, chiseled, or disked early in spring of the fallow season. After one or two secondary

tillage operations with a disk or light tined-cultivator, before mid May, a rodweeder is operated at depths less than 15 cm throughout the summer to control weeds and disrupt capillary continuity. Three to five rod weedings are normally required. Winter wheat is then drilled as early as 1 September. Improper tillage management often delays winter wheat germination and emergence and fails to provide a good soil surface cover for protection against soil erosion during winter (Cochran et al., 1970).

Rodweeding characteristically firms the moist soil under the rodded depth of approximately 15 cm, and creates a dry mulch of low bulk density soil above the rodded depth (Papendick et al., 1973; Pikul et al., 1979). The interface between these two soil layers is usually abrupt. Conserved water at seedbed depth was linked (Papendick et al., 1973) to minimum vapor and liquid flows through the soil mulch. Water content of the expected seedzone is thus maintained through a balance of upward unsaturated flow from deep moist soil and downward flow of water vapor. Other research on heat and water conservation by surface mulching has shown that the heat, liquid, and vapor transport properties of mulch layers are substantially different from the underlying soil (Greb, 1966; Hanks and Woodruff, 1958). Typically mulch layers, as those of rodweeded summerfallowed fields, are dry enough so that vapor movement can be considered the dominant mechanism for water flux.

Diffusion of water vapor on either temperature or water content gradients can be calculated by existing heat and mass flow theory; however, a thorough treatment of vapor flow under field conditions may need to include turbulent mass flow of water vapor in large soil pores. For some soil conditions near the surface Allmaras et al. (1977) found

that tilled layers with > 0.61 fractional total porosity are subject to turbulence effects. In this field study the estimates of turbulence enhanced heat transport in tilled layers corroborated laboratory and theoretical estimates of turbulence effects on vapor transfer in media with similar porosity characteristics. Hanks and Woodruff (1958) showed that mass flow of water vapor in air near the surface is important and indicated that mulches with small voids are more efficient in conserving moisture than mulches with large voids. Farrell et al. (1966) suggest that wind influences cannot be ignored in field evaluations of mulch effectiveness. For a wind speed of 7 m/s surface air can penetrate coarse soils and mulches to a depth of several centimeters. Effective diffusion coefficients for coarse mulches can be as much as 100 times the molecular diffusion. Other theoretical studies also have shown the importance of mass flow near the surface (Kimball and Lemon, 1971; Scotter et al., 1967).

The role of vapor flow in regulating soil moisture at seedzone depths in dryland wheat production areas is not well understood. Little field research has been conducted on this subject and indications are that vapor flow under certain conditions is significant. Farmers of the traditional wheat-fallow area of the Pacific Northwest frequently complain of accelerated water loss from the expected seedzone, before seeding in mid-September to mid-October, especially when a hot, dry August is followed by warm days and cool, clear nights in September. When these apparently excessive water losses occur, wheat germination is delayed until the late fall when the rainy period begins. These management difficulties may be a response to changing diurnal soil heat flux patterns in response to a

seasonal shift of heat flow. Philip (1957) suggested, in an interpretation of his results, that evaporation from the soil is least when the heat flux into the soil is greatest and greatest when the heat flux from the soil is greatest. These theoretical findings of Philip indeed parallel farmer observations and present the paradox that water loss from dry, fallowed soils may be least when, by the usual standards, weather conditions are most favorable for evaporation (seasonally, summer; diurnally, midday).

Evaporative loss must be minimized to assure efficient storage of soil water during the summerfallow period. The rod-weeding tillage implement effectively creates soil conditions that minimize liquid and vapor fluxes and as such is the accepted practice in the Pacific Northwest. However, recent research findings illustrate the high erosive potential of summerfallowed fields that have been pulverized by successive rod weedings during the summer (George, 1982). Clearly the need exists to develop summerfallow tillage systems that minimize the potential for erosion yet create soil conditions that effectively reduce vapor fluxes from the soil during the fallow period.

Strange as it sounds it may also be important to maximize vapor flow to the seedzone during the critical germination and emergence of dryland wheat, especially in marginally dry seedbeds. Lindstrom et al. (1976) characterize the suitability of seedbeds in terms of water potential. Emphasis has recently been placed on drill opener manipulation of the soil micro-environment to facilitate the germination and emergence of wheat. Opener type significantly affects seedling emergence, seed distribution, and soil moisture in the top 5 cm

of soil over winter wheat seed in a summerfallowed production system in the Pacific Northwest (Wilkins et al., 1981). Choudhary and Baker (1981) highlighted, but did not test, the importance of vapor movement in the micro-environment created by direct drilling coulters and covering devices. Improved seedling emergence in dry soils was linked to designs that 1) exploited the limited supply of sub-surface soil moisture by inducing maximum moisture diffusion across the soil-seed interface, 2) closed the surface to prevent convective losses of vapor, 3) maintained a high incidence of surface mulch, 4) physically loosened and shattered the sub-surface soil to assist in rapid root anchorage.

Studies indicate that the role of water vapor in the imbibition of seed may be greater than previously thought, and that capillary and vapor movement of water near the seed as influenced by compaction, and not soil-seed contact, are apparently the controlling factors in imbibition (Rogers, 1979). Collis-George and Melville (1978) modeled water absorption by a swelling seed and evaluated seedbed conditions where vapor transport, as distinct from liquid supply, would dominate wheat seed imbibition. Based on laboratory findings they discussed dry seedbed conditions of Australian wheat, where large quantities of dry stubble straw are incorporated into the soil with the seed. Under these conditions the straw not only competed with the seed as a water vapor sink, but also decreased the thermal conductivity and bulk density so that heat dissipation into the soil may become limiting. Myrold et al. (1981) investigated water potential-water content characteristics of wheat straw and silt loam. A several-fold difference in water content vs. a specific water

potential was found between silt loam and straw. Low rates of heat dissipation by the surrounding soil were purported, by Collis-George and Melville, to accelerate heat accumulation in the seed which is a sink for the latent heat of condensation at the seed surface. As heat accumulates and the seed temperature increases the difference in water vapor concentration between the seed and the supply decreases. A consequence of reduced vapor gradients is a reduction in water vapor flux to the seed.

With current emphasis on reduced tillage systems research is needed to evaluate new tillage implement and drill opener designs as they influence heat and moisture fields. Our understanding of heat and mass flow theory is largely limited to controlled laboratory conditions where research is conducted on uniformly packed homogeneous soil. There are very few reports of field studies on heat and mass transfer that make use of the existing theoretical solutions for combined heat and mass flow. Those few studies often report conflicting results and interpretations. Under dryland farming conditions of the Pacific Northwest, where vapor flux is likely to be the dominant mechanism for water movement during the summer and fall, there is a need for elucidation of heat and vapor flux theory. One such theory, the Philip-de Vries formulation to approximate the influence of moisture movement on the heat transfer in soils, will be used intensively in this thesis.

The total vertical soil heat flux equation of Philip (1957) as used in this paper includes the theoretical evaluation of soil thermal conductivity proposed by de Vries (1963). de Vries theory has frequently been evaluated in the laboratory but field investigations

are few. The Philip-de Vries theory can, however, conveniently be used to study water and heat flow in dry soils, because in a dry soil liquid-flow is extremely slow. This permits the investigator to evaluate both the heat flux and the vapor component of this flux. The theory does not include convective mass flow of soil air, which could be important when soil pores are sufficiently large. An alternate approach for evaluating vapor fluxes is Cary's phenomenological method (1966). Jury and Letey (1979) have recently reconciled Cary's methods with the mechanistic theory of Philip-de Vries.

Sepaskhah and Boersma (1979) compared apparent thermal conductivities measured with a cylindrical heat probe to those calculated with the de Vries model using various water contents at 25°C and 45°C. Their laboratory research strictly adhered to de Vries theory with the possible exception of the trial and error method used to obtain the critical water content that defines air or water as the continuous medium. The de Vries model was satisfactory in this study however, an improvement may be needed to account for enhanced vapor transfer at high temperatures (45°C). In pumice soil Cochran et al. (1967) found good agreement between measured thermal conductivity and thermal conductivity predicted by the de Vries theory. This study deviated significantly from de Vries theory, in that at high water contents the soil solids were considered to be the continuous medium rather than water as proposed by de Vries. Wierenga et al. (1969) analyzed the thermal properties of a Yolo silt loam on the basis of laboratory and field measurements. They reported a favorable agreement of <u>in situ</u> thermal conductivity measurements with thermal conductivity calculated by de Vries theory. However they used an air

shape factor smaller than that postulated by de Vries, an adjustment which will reduce thermal conductivity.

Jackson et al. (1975) conducted experiments in the top 10 cm of a natural field soil to compare measured heat fluxes with those calculated by the methods of Philip. Calculated and measured heat fluxes agreed well at night; but when there were large temperature gradients during the day, calculated heat fluxes overpredicted. Refinements were needed to accurately predict the vapor fluxes due to thermal gradients.

Kimball et al. (1976) used the same data as Jackson et al. (1975) in a comparison of field measured null-alignment heat flux (Kimball and Jackson, 1975) with heat flux calculated by the Philip-de Vries theory. A fair agreement between measured and computed fluxes was obtained only after modifying the de Vries thermal conductivity and ignoring heat transfer due to water vapor movement. (This does not imply that water vapor transfer is not taking place). The authors present a comprehensive analysis of both the theoretical heat flux calculations and previous research work using the Philip-de Vries theory especially de Vries thermal conductivity. They contended that previous investigations have reported general agreement between computed and measured values in tests of de Vries (1963) theory for thermal conductivity, but many of the studies modified the de Vries theory to obtain satisfactory agreement with data for a particular soil. Apparently modifications of the theory are required for reliable predictions of thermal conductivity for individual soils.

Hadas (1977) conducted field and laboratory measurements to compare Philip-de Vries model of heat and moisture transfer with

measured values. Hadas adheres to the de Vries theory for calculating thermal conductivity. The only assumption peculiar to his analysis was that the test soil particle shape was ellipsoidal. Good agreement (within 5%) was obtained between predicted and measured thermal conductivity except for those times of the day when the thermal gradient was reversed (from the deeper soil outward toward the surface). It was also found that the Philip-de Vries model quite accurately predicted the transfer of heat by vapor under steady state conditions, but that it underestimates it under nonsteady state conditions.

Hadas concluded that the Philip-de Vries model of heat and water transfer provides reasonable prediction when it is used consistently with the assumptions it was based upon. He states that the discrepancies which have been reported are due to difficulties in accurately measuring all the parameters involved. He points out that the Philip-de Vries model fails whenever conditions prevail such as wind gusts, thermal gradient reversals, and air mass movement caused by air pressure changes because the model did not conceptually include these effects. Hadas suggests that correcting equations based on studies of the convective heat and moisture processes be applied to the existing theory. Since Hadas' only assumption was about the shape of the particles he indicates that there is no need to calibrate the soil in order to make it comply with the theory as suggested by Kimball et al. (1976).

The foregoing discussion indicates that soil heat flow cannot be predicted accurately, and that controversy exists regarding the predictive abilities of the de Vries thermal conductivity. The cautious

investigator must determine the suitability of the Philip-de Vries theory on a soil-by-soil basis, and considerable field effort is necessary to attain confidence in relating heat flow to soil treatment.

The objective of this research was to test the Philip-de Vries soil heat flux theory in the field on a wet and dry Walla Walla silt loam. A second objective was to separate the vapor heat flux component from the total soil heat flux and use this refinement to predict soil water changes at shallow depths under relatively dry soil conditions. Field testing of the Philip-de Vries theory will serve: 1) to evaluate the effects of tillage and drill opener practices on soil physical properties that could affect vapor fluxes; 2) to further expand the body of knowledge about measured and calculated heat and mass flow.

MATERIALS AND METHODS

Plot Preparation

Field plots were established during September of 1979 at the Columbia Plateau Conservation Research Center located 14.5 km northeast of Pendleton, Oregon. The Research Center lies on the eastern fringe of the traditional wheat-fallow region of Oregon (Leggett et al., 1974). Peas, wheat and other small grains are the important dry-farmed crops. Annual precipitation at the research site is 400 mm occurring mostly as rain during October through June. Soil at the site is a Walla Walla silt loam (member of the coarse, silty, mixed mesic family of Typic Haploxerolls). Slope at the site was nearly zero.

Stephens winter wheat (Triticum aestivum L.) was harvested during August of 1979 leaving a straw residue of 9,000 kg/ha. A 50 m-by-25 m site was selected in a uniform stand of stubble 30-cm tall. One-half of the area was burned leaving two 25 m-by-25 m plots. Stubble burning produced a surface completely free of all harvest residues and subsequent winds carried off most of the ash. Chaff was redistributed in the standing stubble plot to produce a uniform interrow coverage of the soil surface. Weeds were controlled as needed on both plots with 0.6 kg/ha glyphosate (Round-Up) during the fall and spring. No tillage was performed.

Instrumentation of both plots, in the manner described in the following sections, was completed during October 1979. Although the measurements reported here were not obtained until July 16, 1980, it was necessary to install instruments in 1979 before winter to

accommodate a study of frost penetration and persistence as influenced by crop residue management (Pikul, 1982). The burned stubble plot was irrigated on July 10 for the purpose of comparing calculated heat flow in soils with markedly different water contents. Hereafter the burned stubble plot will be called the wet soil treatment and the stubble covered plot will be called the dry soil treatment.

Soil Temperature

Soil temperature at each depth was sensed by duplicate temperature probes, each of which averaged the signal from three thermocouples. Probes were constructed as follows. Three copper-constantan junctions wired in parallel were inserted into a 45-cm long tube 4.5 mm in diameter. This tube had a low thermal conductivity characteristic of cellulose acetate butyrate. The three thermocouple junctions, spaced 20, 32, and 45 cm from the end of the tube, were imbedded in a high thermal conductivity epoxy that protruded from the wall of the tube at each junction.

Temperature probes were inserted into the soil from the face of a trench after a relief hole (smaller diameter than the tubing used to construct the probe) was drilled using a drilling template to assure an accurate depth parallel to the surface. Epoxy at each junction ensured good thermal contact with the soil. Depths of thermocouples were 0.25 cm, 1-cm increments from 1 to 5 cm, 2-cm increments from 7 to 25 cm, 30, 35, 40, 50, 60 cm. This installation procedure ensured that no thermocouple junction was less than 20 cm from the disturbed soil of the trench area.

For the time period beginning 2000, July 15 to 0800, July 17, soil temperatures on both plots were automatically scanned and recorded at 30-minute intervals. In preparation for soil heat-flux analysis the raw soil temperatures were first smoothed as a function of time using a Fourier analysis (Panofsky and Brier, 1968). To represent data in a Fourier Series the input data must be periodic (with the same beginning and ending points) on evenly spaced intervals. During the summer when soils are warming soil temperatures recorded at midnight at shallow depths (less than 30 cm for this soil) rarely have the same value from day-to-day.

To overcome the difficulty of smoothing non-periodic soil temperature measurements near the surface a temperature recording and smoothing scheme was developed. By using this Fourier-smoothing scheme it was possible to smooth soil temperatures, that did not exhibit the same midnight temperature, at any depth. At each depth of temperature measurement a computer program searched the buffer data before and after July 16 for soil temperatures that matched within 0.2°C. Buffer data was used to describe the temperature data from 2000 to 2400 on July 15, and from 0030 to 0800 on July 17. By using the buffer data exact matches of starting and ending point temperatures at a given depth were possible in most cases. Soil temperatures at each measurement depth were then described as a sum of sines and cosines in a Fourier Series as:

$$T_i(j) = a_o + a_1\cos(\omega j) + a_2\cos(2\omega j) + \ldots + a_K\cos(k\omega j) + b_1\sin(\omega j) + b_2\sin(2\omega j) + \ldots + b_K\sin(k\omega j) \qquad [1]$$

where T_i = soil temperature at depth i,

ω = angular frequency defined as $\frac{2\pi}{N}$,

N = the number of observations,

j = time counter (for 1, 2, ... , N),

$$a_o = \frac{1}{N} \sum_{j=1}^{N} T_j$$

$$a_k = \frac{2}{N} \sum_{j=1}^{N} T_j \cos(jk \cdot \frac{2\pi}{N}) \text{ for the kth harmonic coefficient,}$$

$$b_k = \frac{2}{N} \sum_{j=1}^{N} T_j \sin(jk \cdot \frac{2\pi}{N}) \text{ for the kth harmonic coefficient.}$$

By using the form of Equation [1] the first derivative was readily obtained and $(dT/dt)_{ij}$ was calculated for all depths and times. In a later section $(dT/dt)_{ij}$ is used in the calculation of heat flux by the null-alignment method. Examples of smoothed soil temperatures for midnight to midnight at 0.25, 2, 5, 11, 17 and 35 cm for the wet and dry plots are shown in Figure 1 and 2, respectively. Finally the 0.25- to 60-cm soil-temperature-profile at each 30-min interval was smoothed with depth using a cubic-spline-fitting technique (Kimball, 1976; Kimball, 1975). Smoothing of each temperature profile over depth allowed an evaluation of the temperature gradient, $(dT/dz)_{ij}$, at the point of temperature measurement.

Meteorological Measurements

To characterize weather conditions during the 24-hour study on 16 July, meteorological measurements were taken at 30-min intervals on both plots. Reflected and incident shortwave radiation at 1 meter was measured using inverted and upright Eppley radiometers. Air temperature

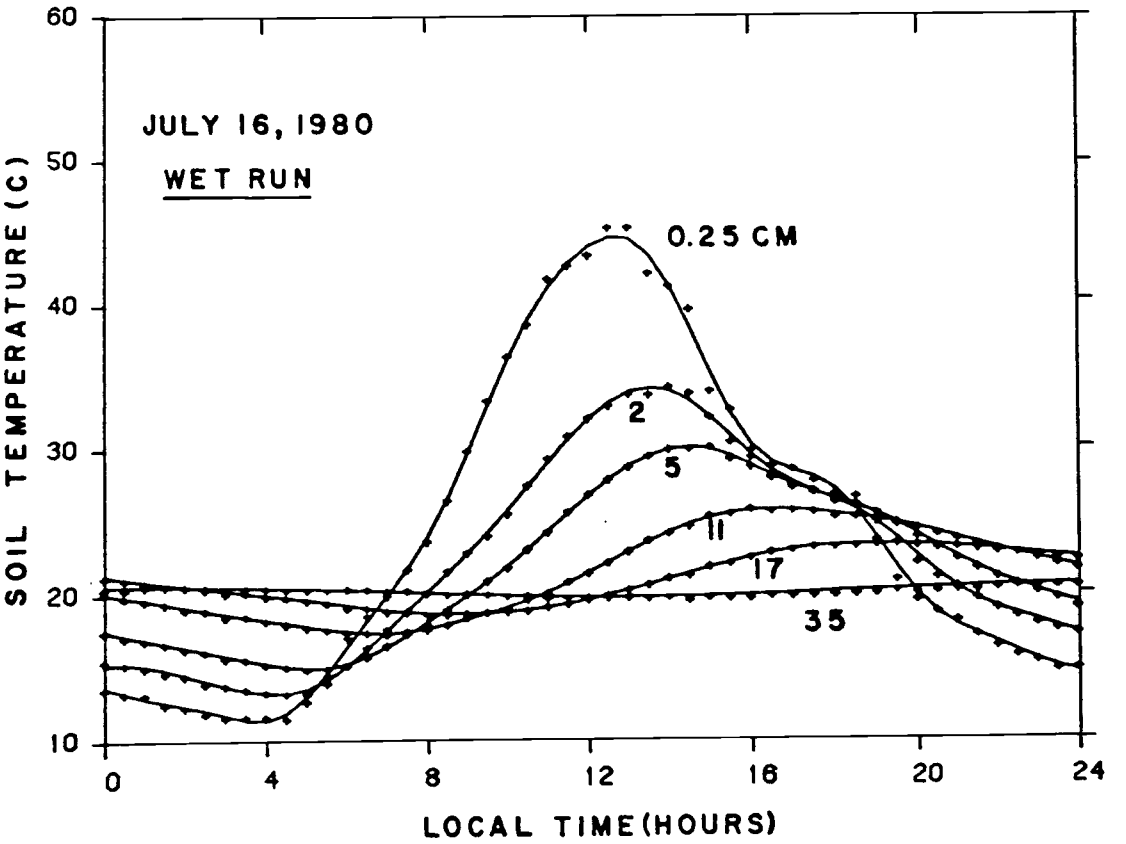

Figure 1. Diurnal wave of soil temperature at 0.25, 2, 5, 11, 17 and 35 cm on the wet Walla Walla silt loam.

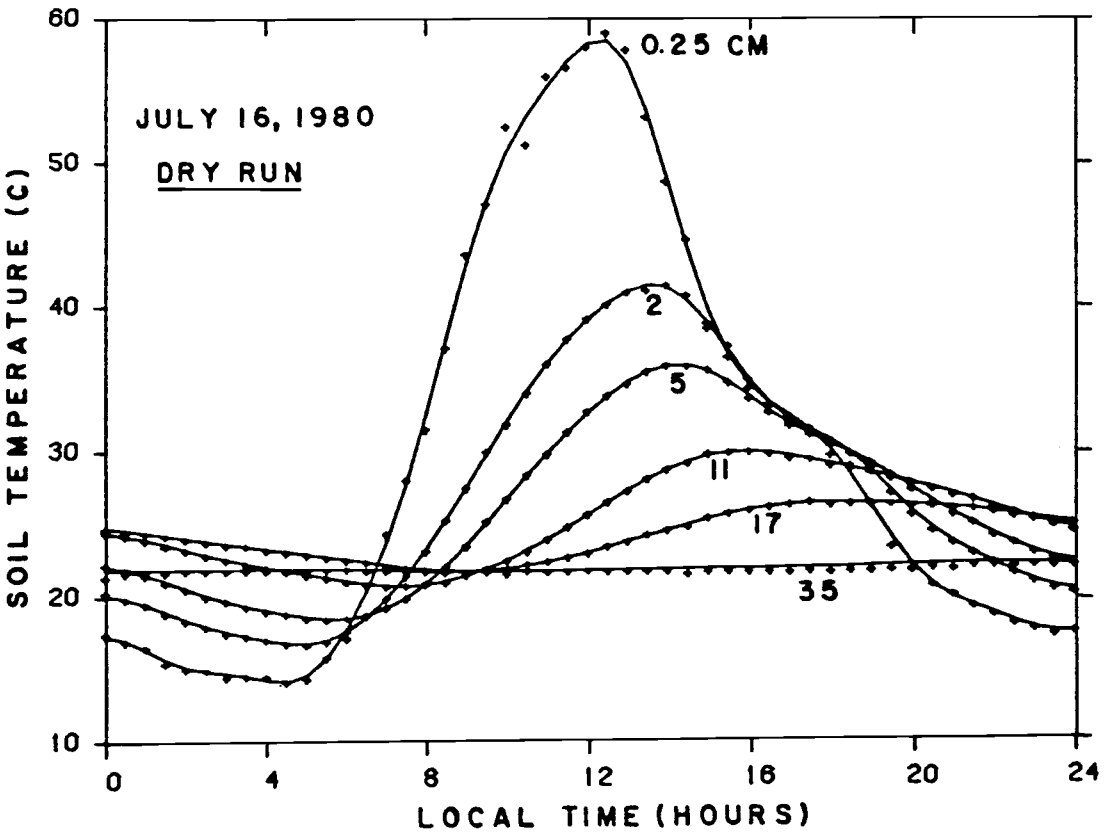

Figure 2. Diurnal wave of soil temperature at 0.25, 2, 5, 11, 17 and 35 cm on the dry Walla Walla silt loam.

profile measurements were made at 15 and 150 cm. Wind run and relative humidity were obtained at 150 cm using a 3-cup anemometer and recording hygrothermograph, respectively.

Soil Water Measurements and Hydraulic Properties

Soil water content in the surface-to 11-cm profile was determined gravimetrically at 2 and 4 hour intervals for the wet and dry plots, respectively. Water content samples were taken 3 meters from the soil temperature probe installations. A composite sample consisting of three subsamples was collected at each sampling time. The midpoints of these samples were at 0.25, and at 1-cm increments in the 0.5- to 10.5-cm range. This composite sample was used to determine bulk density and gravimetric water. Soil water content in the profile beyond 11 cm was sampled once at midday. Samples were obtained at 5-cm increments from 10 to 40 cm and 10-cm increments from 40 to 60 cm. Pikul et al. (1979) gave details of the sampling procedure for gravimetric water and soil bulk density.

Duplicate sets of tensiometers were placed on both plots at 15, 20, 25, 30, 40, 50 and 60 cm. Manometer boards were read at the times of gravimetric soil sampling. Hydraulic head readings were used to detect soil water changes in the 15- to 60-cm portion of the soil profile where gravimetric water content was not sampled at close time intervals. During the 24-hour sampling period hydraulic heads indicated little or no change in water content at these deeper depths.

In preparation for heat and water flux analysis, gravimetric water contents, θg, were converted to a volumetric basis, θ:

$$\theta_{ij} = \theta g_{ij} \times \rho b_i \qquad [2]$$

Bulk density values, ρb, for the 0.25-to 60-cm profile were obtained from a depth function generated by a cubic spline (Fig. 3). Volumetric water content at each sampling depth was then smoothed as a function of time using a cubic spline. Using these time functions, a value of θ at 30-min intervals was generated for each soil-water sampling depth in the 0.25-to 10.5-cm profile for the 24-hour study period. Examples of smoothed θ at several depths for the wet and dry plots are shown in Figs [4a and 4b], respectively. These diurnal changes in soil water are similar to those found by Jackson (1973). A 0.25-to 60-cm-water-content-profile at each 30-min interval was then smoothed as a function of depth using a cubic spline. Time and depth smoothing of each water profile allowed evaluation of water content, θ, and water-content gradient, $d\theta/dz$ at the depths and times corresponding to soil temperature measurements.

A characteristic curve for the 60-cm soil profile (Fig. 5a) was developed as a composite of coordinate pairs for soil depths $\leq$ 45 cm. Both tensiometer versus volumetric water and psychrometric water potential versus volumetric water were used. In situ soil water potential for $\theta > 0.22$ cm^3cm^{-3} for this test soil were taken from tensiometric data for 23 and 30 cm (Allmaras, 1982), and for 2, 5, and 9 cm (Pikul, unpublished). Disturbed soil cores at 15, 23, 31, and 45 cm were used for psychrometric water potentials for $\theta < 0.22$ cm^3cm^{-3} (Allmaras, unpublished). The use of disturbed cores for these depths was not considered a serious limitation. Soil moisture retention in the low potential range is due primarily to adsorption which is correlated with specific surface rather than structure. The Walla Walla soil exhibits a uniform particle size distribution throughout the 45-cm

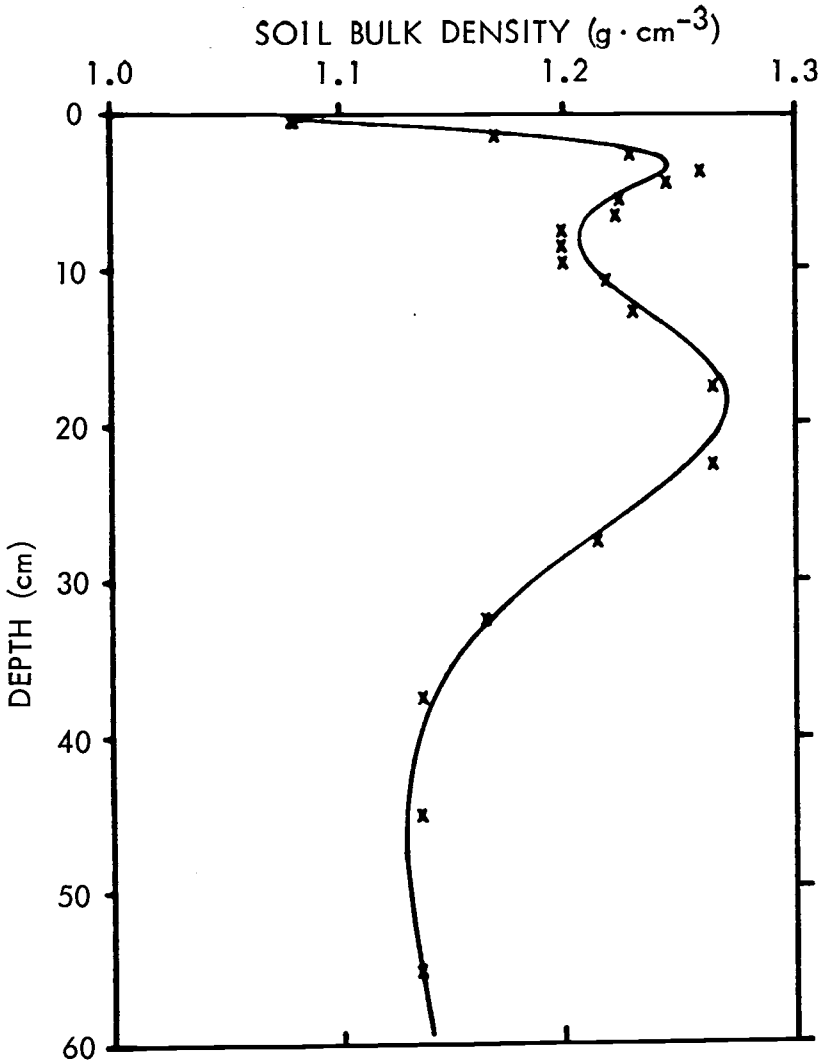

Figure 3. Soil bulk density for the untilled Walla Walla silt loam test site.

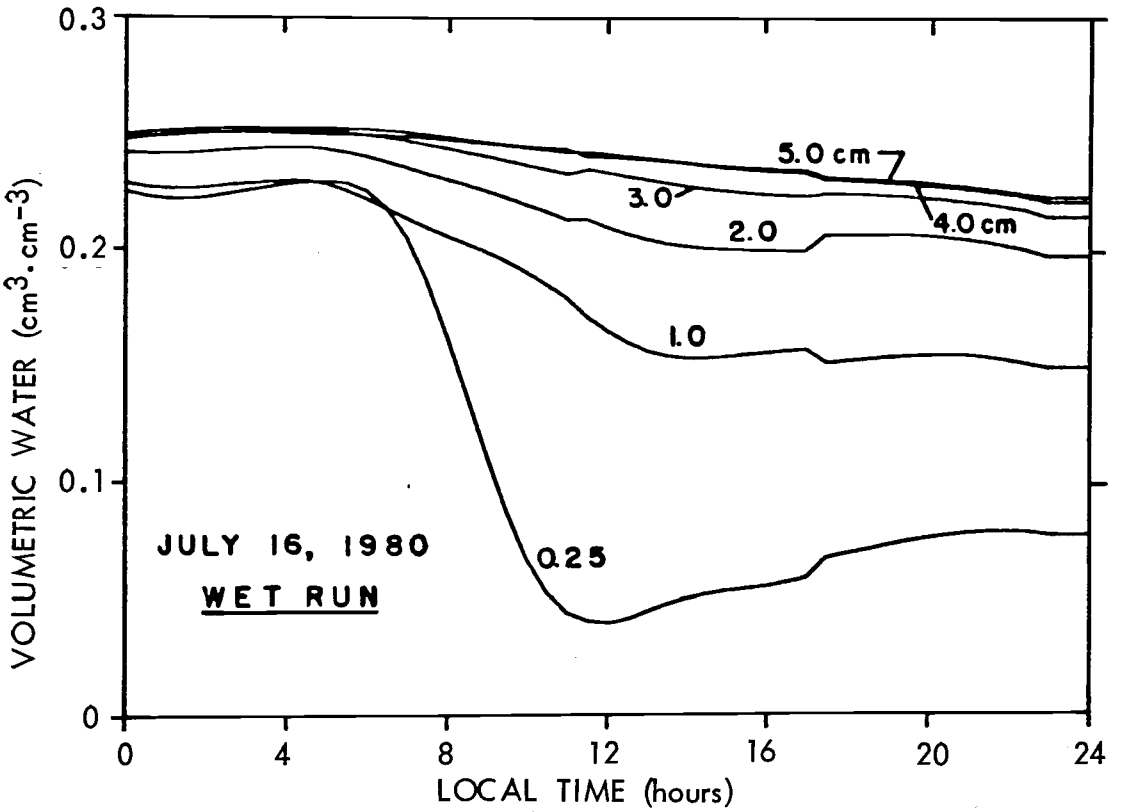

Figure 4a. Diurnal volumetric water content at 0.25, 1, 2, 3, 4, and 5 cm on the wet Walla Walla silt loam.

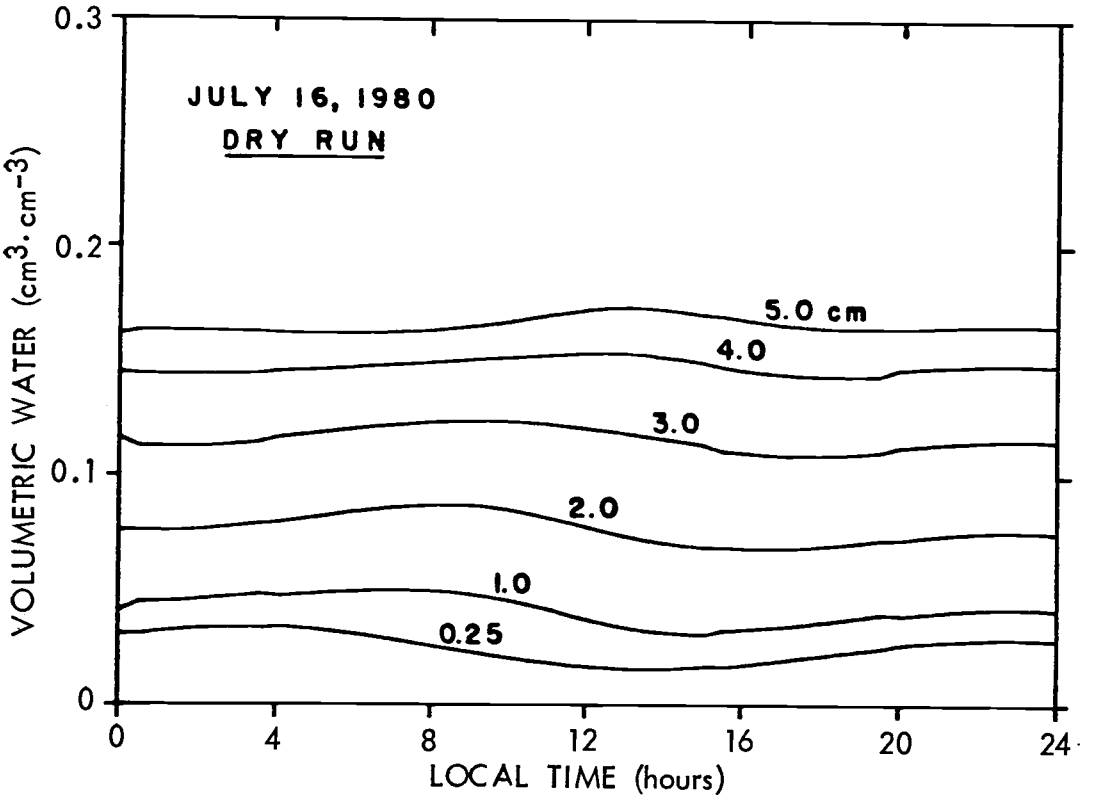

Figure 4b. Diurnal volumetric water content at 0.25, 1, 2, 3, 4, and 5 cm on the dry Walla Walla silt loam.

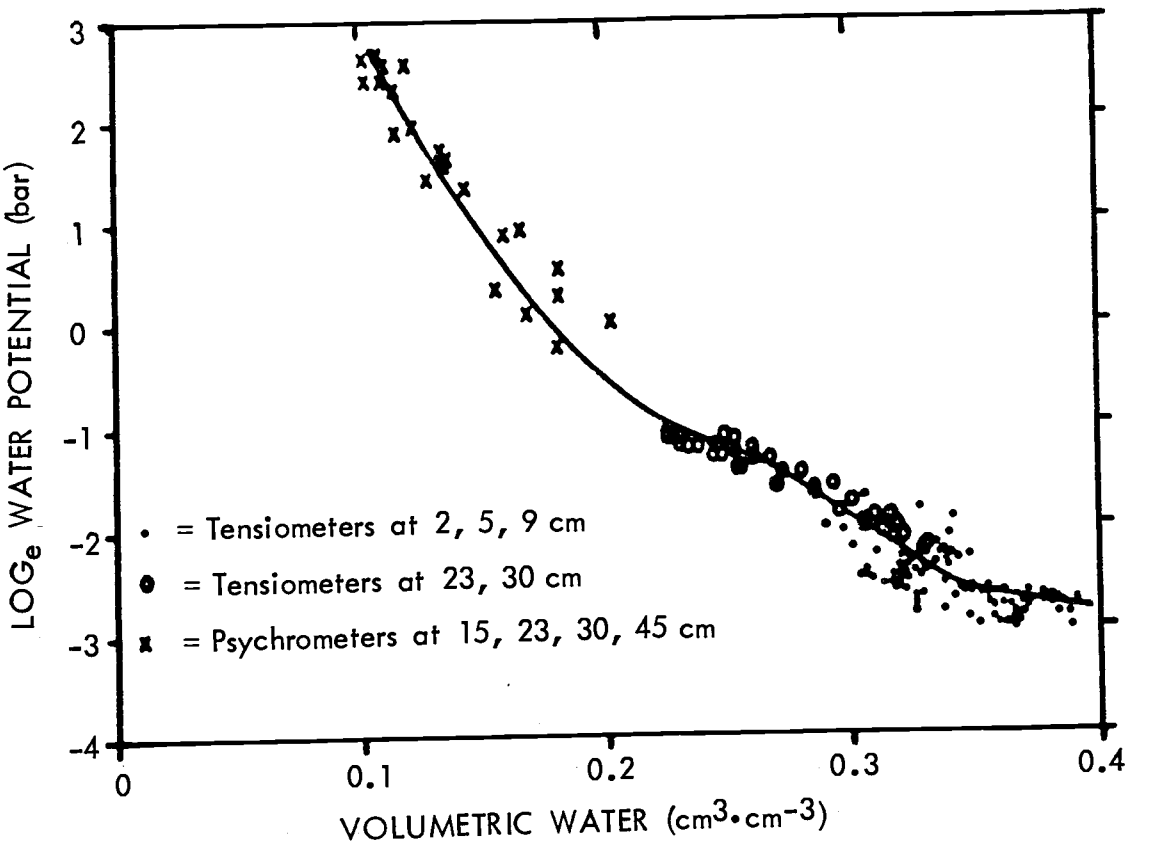

Figure 5a. Soil water desorption characteristic in the 2 to 45-cm layer of the test Walla Walla soil. (Water potential plotted as positive values).

profile (Table 1). Volumetric water versus the natural log of water potential in bars was fitted to a cubic spline (Fig. 5a). The water release curve of Fig. 5a was then used in a modified form of the Marshall pore-interaction model to calculate hydraulic conductivity (Green and Corey, 1971). This method requires that one point on the calculated hydraulic conductivity curve be matched to an experimentally measured hydraulic conductivity value. The matching point for this work was an average of four replicates of saturated hydraulic conductivity at 15 cm taken with a double tube infiltrometer (Bouwer, 1962). Hydraulic conductivity as a function of volumetric water content is shown in Fig. 5b. Also shown in Fig. 5b are field determined conductivities at 30 cm (Allmaras, 1982) for intermediate water contents.

Measured Water Profile Changes

The change in water content of soil slabs in the upper 11 cm of soil was calculated from volumetric water content measurements. The boundaries of these slabs are 0.25, 1, 2, 3, 4, 5, 7, 9, and 11 cm. The change in water content during a 24-hour period was found as:

$$Cw_{i+1}^{i} = \sum_{j=2}^{49} (Z_{i+1} - Z_i) \cdot \left[\left(\frac{\theta_{ij} + \theta_{(i+1)j}}{2} \right) - \left(\frac{\theta_{i(j-1)} + \theta_{(i+1)(j-1)}}{2} \right) \right] \qquad [3]$$

..... (cm)

where Cw is the change in water content of a slab defined by upper and lower boundaries i and $i+1$, respectively, for time j. The above sign convention provides for an increase to be indicated by a positive sign and a decrease to be indicated by a negative sign. The net change as

Table 1. Particle size distribution, percent quartz, and weighted thermal conductivity for the test Walla Walla silt loam. (Soil analysis by the S.C.S., Lincoln, Neb.)

Fraction	% of total soil	% quartz	% other mineral	Quartz % of total soil
		0- to 15-cm		
coarse silt	32.4	55.0	45.0	
very fine sand	12.4	40.0	60.0	
fine sand	4.2	19.0	91.0	
		15- to 30-cm		
coarse silt	31.5	50.0	50.0	
very fine sand	12.7	36.0	64.0	
fine sand	4.4	18.0	82.0	
		30- to 46-cm		
coarse silt	32.5	57.0	43.0	
very fine sand	14.7	39.0	61.0	
fine sand	4.0	18.0	82.0	
		Average for 0- to 46-cm profile		
coarse silt	32.13	54	46	17.35
very fine sand	13.27	38.33	61.67	5.09
fine sand	4.2	18.33	81.67	0.77

		Weighted thermal conductivity	
Component	% of total soil	Thermal conductivity	Weighted thermal conductivity
quartz	23.21	20.4	4.73
other mineral	74.79	7.0	5.24
organic matter	2.00	0.6	0.01
			9.98 mcal/cm•sec•C

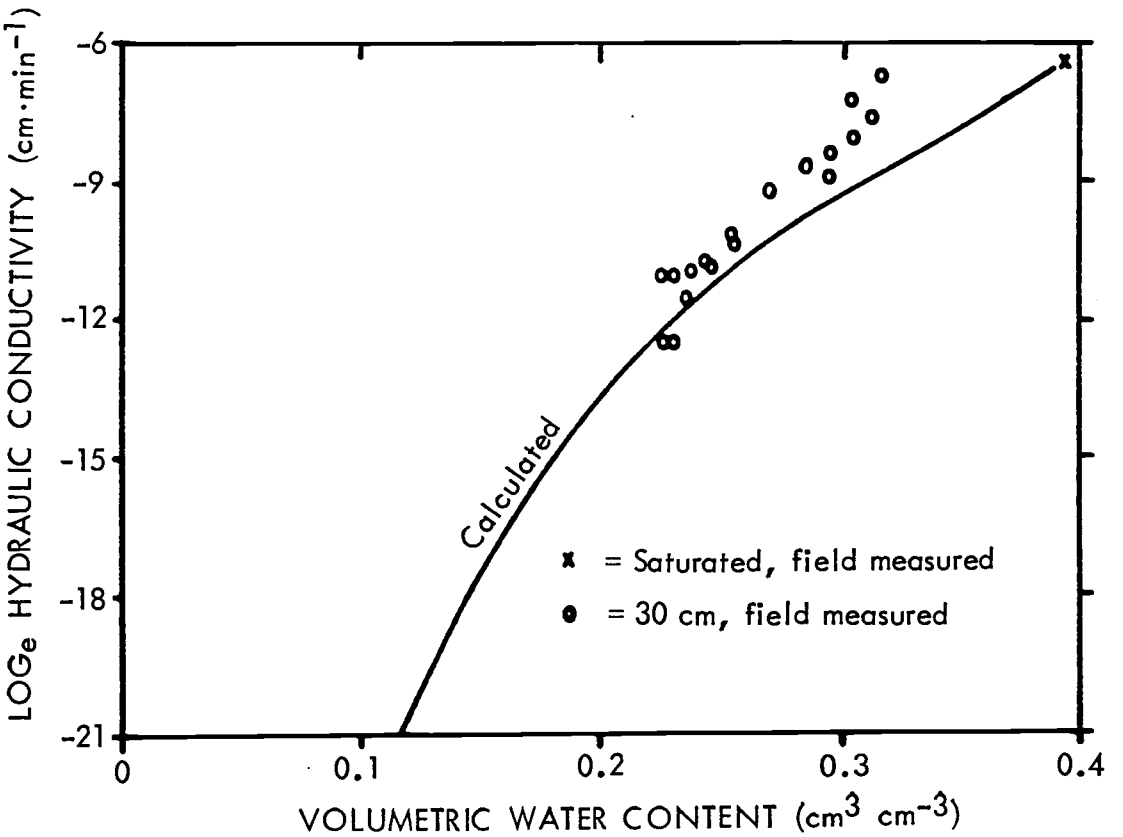

Figure 5b. Calculated and field measured hydraulic conductivity for the test Walla Walla silt loam.

found by Equation [3] will include water movement in both the liquid and vapor phases along temperature and potential gradients. For this equation and others appearing in the text the units will be indicated in parenthesis following the equation.

Isothermal Liquid Water Flow

Net flow of liquid water, q, into and out of a soil slab boundary, $_i$, for each 30-min interval, n, was calculated using the Darcy equation:

$$q_i = -30K(\theta)_{(j+\frac{1}{2})i} \cdot \left(\frac{dH}{dz}\right)_{(j+\frac{1}{2})i} \ldots\ldots \text{ (cm/30-min)} \qquad [4]$$

where $_{(j+\frac{1}{2})}$ designates the hydraulic conductivity, K, and hydraulic head gradient, $\frac{dH}{dz}$, at a mid-time interval. Average flow for the time interval is obtained by multiplying by 30 min per interval. To account for the change in storage of each layer during the measurement period the flow into and out of a slab was summed over time:

$$C_{1\,i+1}^{\,i} = \sum_{n=1}^{48} [q_i - q_{i+1}] \ldots\ldots \text{ (cm)} \qquad [5]$$

The sign convention is positive for a water gain. Appendix 1 illustrates the method used to obtain dH/dz.

DISCUSSION OF HEAT FLUX

Null-Alignment Heat Flux

Measured soil heat flux was determined by the null-alignment procedure (Kimball and Jackson, 1975). It will be considered the standard for calibration of calculation methods. This calibration method requires soil moisture and temperatures measured over small increments of time and depth and an initial estimate of thermal conductivity at some reference depth where thermal conductivity changes little during a day. Kimball and Jackson used a reference depth of 20 cm.

In this study a reference depth of 35 cm was selected based on the propagation of the daily temperature wave. At 35 cm (Fig. 1 and 2) there is an approximate amplitude of 1°C on the wet plot and virtually no temperature change on the dry plot. Tensiometers at 30 and 40 cm indicated no water movement during the measurement period. Thus, the stability of temperature and water regimens at 35 cm, projects no large changes in soil thermal conductivity at the reference depth, of 35 cm. An initial estimate of thermal conductivity at the reference depth, λr, of 2.5 mcal/cm•C•sec was used to calculate reference-depth soil-heat flux, G_{rj}:

$$G_{rj}=-\lambda_r\left(\frac{dT}{dz}\right)_{rj} \ldots\ldots \text{(mcal/cm}^2\text{•sec)} \qquad [6]$$

The minus sign establishes a convention of positive downward depth, z, and positive downward heat flux whenever a warmer temperature is above a cooler temperature. For those times of the day when zero temperature gradients existed, heat flux for all depths above the reference depth was calculated using a calorimetric accounting:

$$G_{ij}=G_{(i+1)j}+0.25\cdot(H_{(i+1)j}+H_{ij})\cdot((\frac{dT}{dt})_{(i+1)j}+(\frac{dT}{dt})_{ij})\cdot(Z_{i+1}-Z_i)$$

$$\ldots\ldots \text{ (mcal/cm}^2\cdot\text{sec)} \qquad [7]$$

A soil slab of thickness ΔZ which has more heat flowing into the top, $_i$, than out of the bottom, $_{i+1}$, will increase in temperature with time, t. The rate of temperature increase is proportional to the heat flux difference, ΔG, between the bottom and top and inversely proportional to the slab thickness. The constant of proportionality is the volumetric heat capacity, H. The constant 0.25 in Equation [7] results from averaging upper and lower heat capacity and temperature change.

Heat capacity was computed from measurements of bulk density and moisture content using Equation [8] developed by de Vries (1963):

$$H_{ij}=10^3(0.46Xm_i+0.60XO_i+Xw_{ij}) \ldots\ldots \text{ (mcal/cm}^3\cdot\text{C)} \qquad [8]$$

where $Xm_i = \frac{\rho b_i}{\rho p} - Xo_i$ is the volumetric fraction of mineral matter,

$Xo_i = (\frac{Or}{1.3})/(\frac{1-Or}{\rho p}).\frac{\rho b_i}{\rho p}$ is the volume fraction of organic matter, and

$Xw_{ij} = \theta_{ij}$ is the volumetric fraction of water.

Measurements of particle density, ρp, were made using air and water picnometers. An average value of 2.657 g/cm^3 is used as an average particle density for the soil profile. Percents of organic matter, Or, on a dry weight basis were obtained from measured total soil carbon and an assumed 58% C in organic matter. A depth function of organic matter was obtained using a cubic spline (Fig. 6). The density of organic matter was taken as 1.3 g/cm^3 (de Vries, 1963). This would be justified since no coarse fragments of soil incorporated straw were

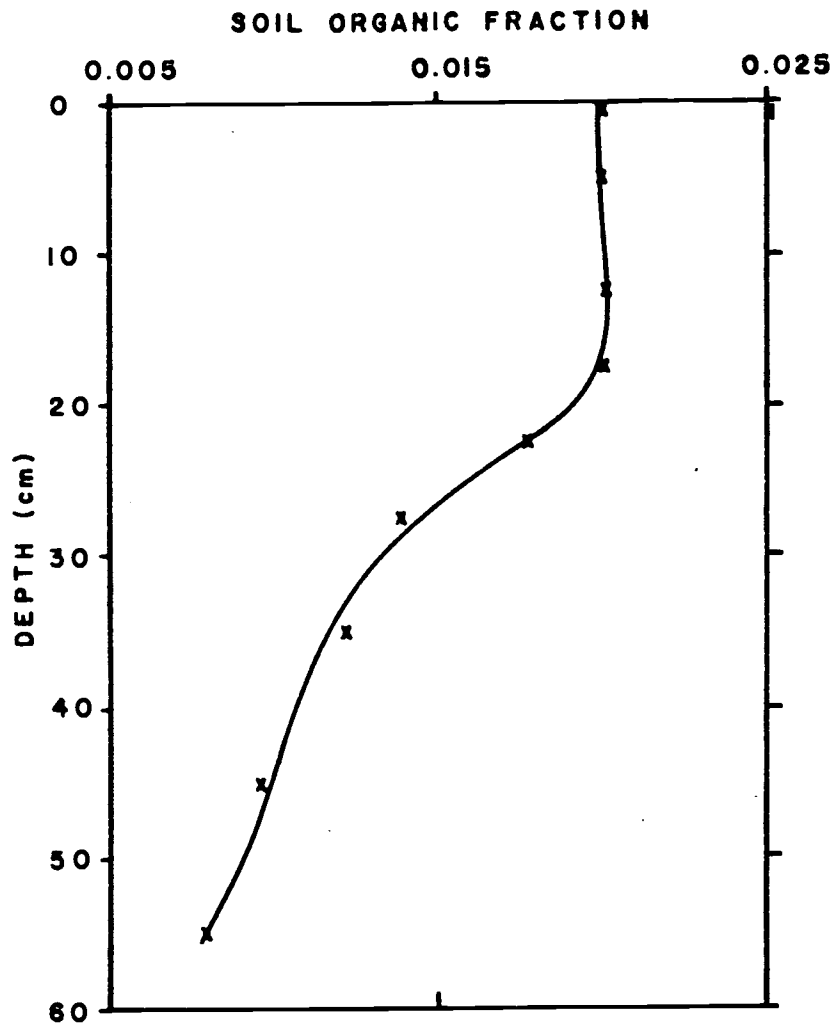

Figure 6. Soil organic matter for the Walla Walla silt loam test site.

found at any depth or time sampling. Soil carbon was measured 2 years after the last residue incorporation.

After the heat fluxes were estimated, zero temperature gradients were then used to force a null-alignment of zero calorimetric heat flux with zero temperature gradient. From this procedure a better estimate of thermal conductivity at the reference depth, λ_{rj}, was determined for each time of day in which a zero temperature gradient was found using Equation [6]. Another advantage of a deep reference depth in the profile is that an average of at least 20 estimates of thermal conductivity were available to recalculate heat flux for all depths and times using Equations [6] and [7].

In this study a large range of null-aligned reference depth thermal conductivities (NARDTC) was found for those profiles exhibiting zero-temperature gradients. A complete listing of time, depth of zero temperature gradient (null point) and resulting NARDTC's is shown in Table 2 and Figs. 7 and 8. For reasons stated earlier this fluctuation of thermal conductivity at 35 cm was unexpected. Furthermore, for the existing temperature and water regimen at 35 cm, the de Vries physical model for computing soil thermal conductivity (discussed in the next section) did not predict this magnitude of change. Computed mean daily thermal conductivities for the wet and dry plots were 2.271 ($S_{\bar{x}}$ = .005) and 2.364 ($S_{\bar{x}}$ = .002) mcal/cm·sec·C, respectively.

There is no physical basis for a five-fold diurnal change in the thermal conductivity at 35 cm (as measured on the dry plot), and there may be several explanations for these apparent anomalous NARDTC's. Kimball and Jackson (1975) suggest criteria for the selection of null points to provide zero heat fluxes at known depths in the profile.

Table 2. Time, depth of zero temperature gradient (null point), and null-alignment reference depth thermal conductivity for the wet and dry field plots.

Wet treatment			Dry treatment		
Time	Null point depth (cm)	λ_{35} [1/]	Time	Null point depth (cm)	λ_{35} [1/]
0000	20.2	2.395	0000	15.1	2.223
0030	20.7	2.233	0030	15.4	1.748
0100	21.4	1.980	0100	15.9	1.438
0130	22.1	1.722	0130	16.6	1.362
0200	23.0	1.533	0200	17.4	1.615
0230	23.9	1.502	0230	18.1	2.080
0300	24.8	1.613	0300	18.6	2.433
0330	25.7	1.788	0330	18.9	2.350
0400	26.9	1.908	0400	19.3	1.787
0430	28.1	1.958	0430	19.8	1.203
1900	6.1	2.085	0500	20.4	1.147
1930	7.5	2.052	0530	21.1	1.735
2000	9.1	2.335	1800	2.5	5.502
2030	10.8	2.063	1830	4.0	5.177
2100	12.1	1.642	1900	5.7	4.872
2130	13.2	1.115	1930	7.0	4.710
2200	14.2	0.728	2000	8.2	3.868
2230	15.0	0.608	2030	9.5	2.625
2300	15.8	0.785	2100	10.9	1.815
2330	16.5	1.173	2130	12.0	1.952
2400	17.2	1.608	2200	12.9	2.508
			2230	13.8	2.93
			2300	14.6	2.91
			2330	15.3	2.56
			2400	15.7	2.103
Average λ_{35} for null Points > 15 cm ----------		1.708	Average λ_{35} for null Points > 15 cm ----------		1.842

[1/] mcal/cm·sec·C

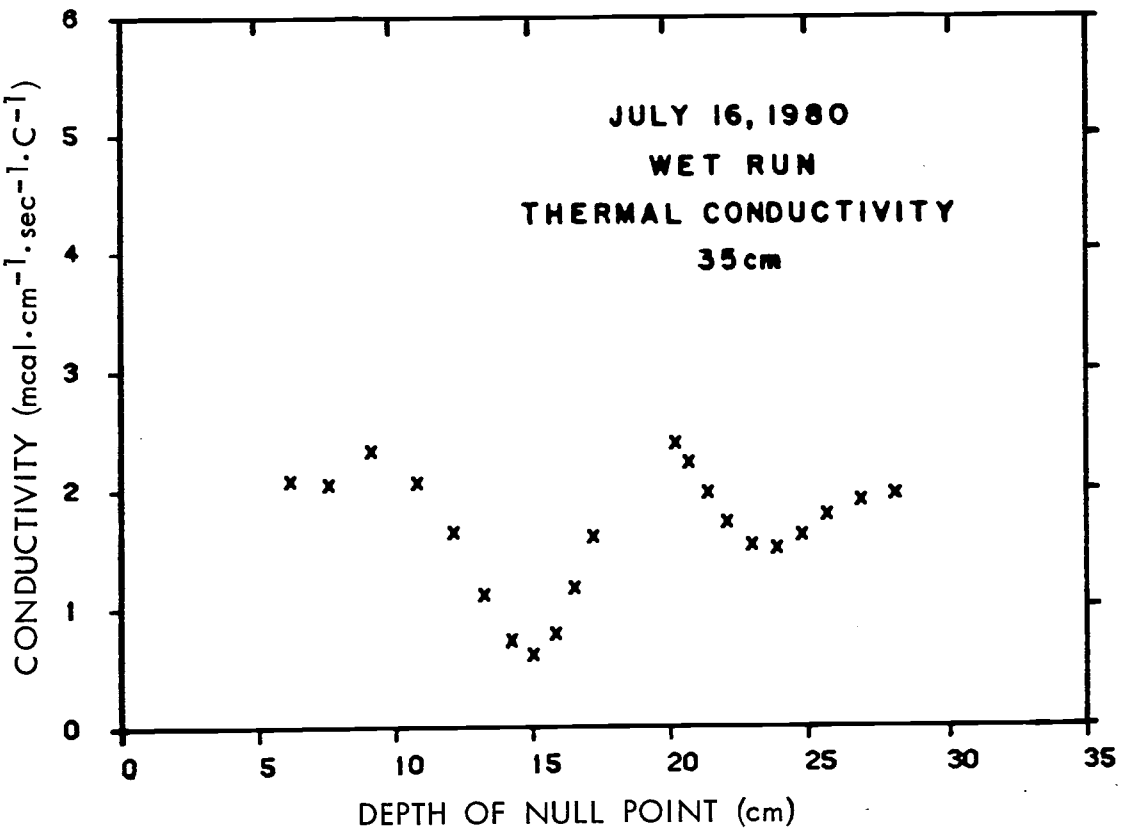

Figure 7. Depth of null point and resulting null-aligned 35 cm soil thermal conductivity for the wet treatment.

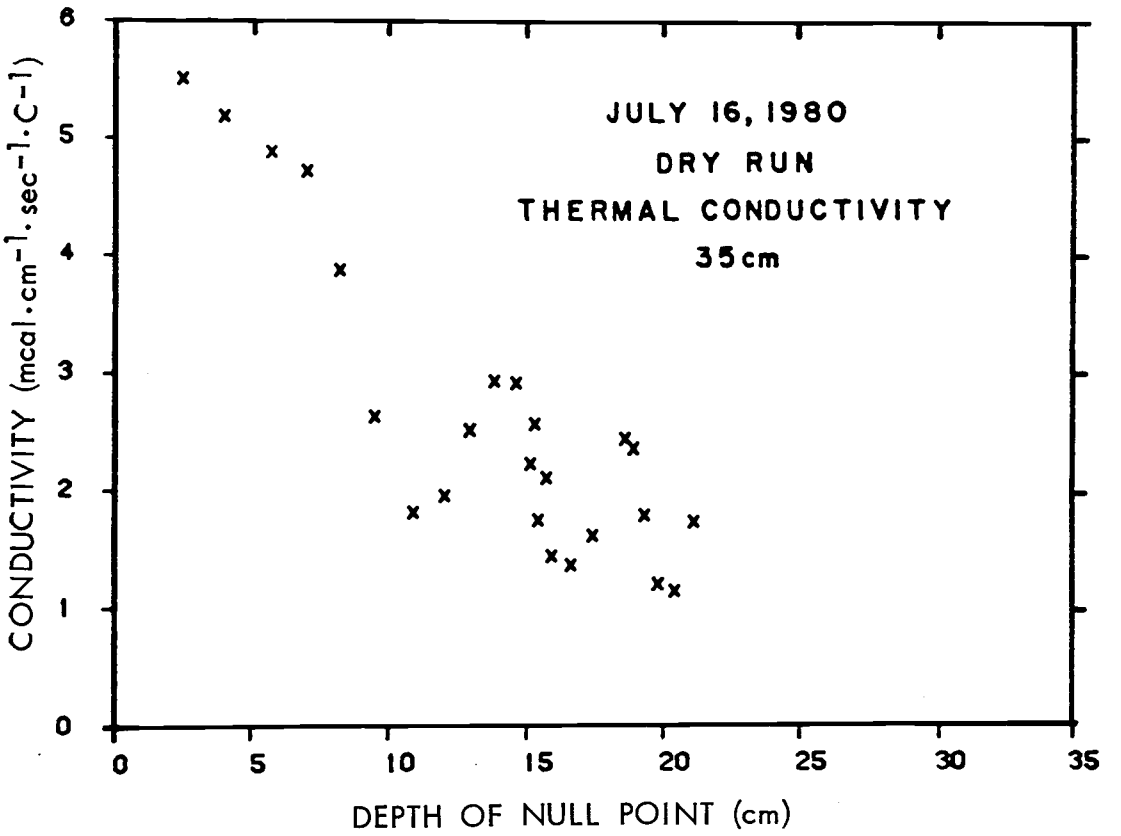

Figure 8. Depth of null point and resulting null-aligned 35 cm soil thermal conductivity for the dry treatment.

First, a null point should be well-defined. Second, heat movement due to water or water-vapor movement must be negligible. They state that this second criteria is not very restrictive because heat movement due to moisture movement can safely be assumed negligible as long as liquid movement is less than 1 mm/hr, and no steep moisture-content gradients exist at the null point depth.

In response to the first criteria requiring well defined null points an index of curvature (Swokowski, 1978) was used to classify the nature of the curve at the null point (dT/dz=0). An example of this comparison is shown in Fig. 9. For a given index (for example .04) of curvature at dT/dz=0, thermal conductivity at 35 cm varied over a wide range. This analysis suggested that a well defined null point (dT/dz=0) had little value as a decision criterion for accepting or rejecting a NARDTC. It must be assumed that the soil temperatures and gradients were precisely measured.

A more physically based criterion is the absence of heat movement at the null point due to water or water vapor movement. If this is not true then an alignment of dT/dz=0 with G=0 at the null point will produce erroneous NARDTC's. Figures 7 and 8 show the relation of NARDTC's as a function of the corresponding null-point depth for the wet and dry treatments, respectively. The wet plot shows a close clustering of points about a mean NARDTC of 1.66 mcal/cm•sec•C, however the standing stubble plot is marked by several NARDTC's that range far beyond a clustering at 2.0 mcal/cm•sec C. As a means of comparison the water profile and temperature profile for one outlying NARDTC at 1900 hours is shown in Figures 10 and 11 for the wet and dry treatment, respectively.

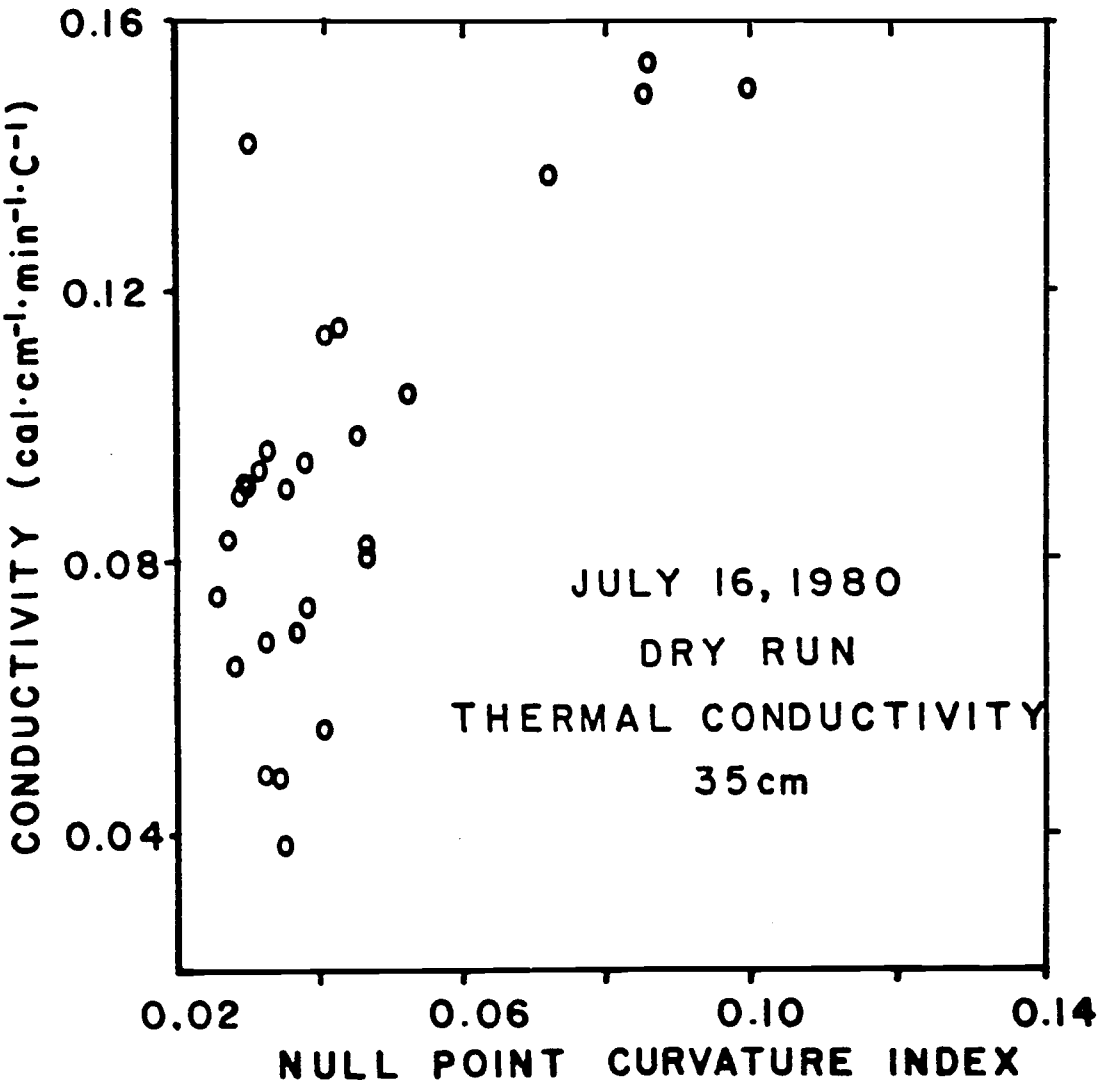

Figure 9. Null point (dT/dz = 0) curvature index and 35-cm soil thermal conductivity for the dry treatment.

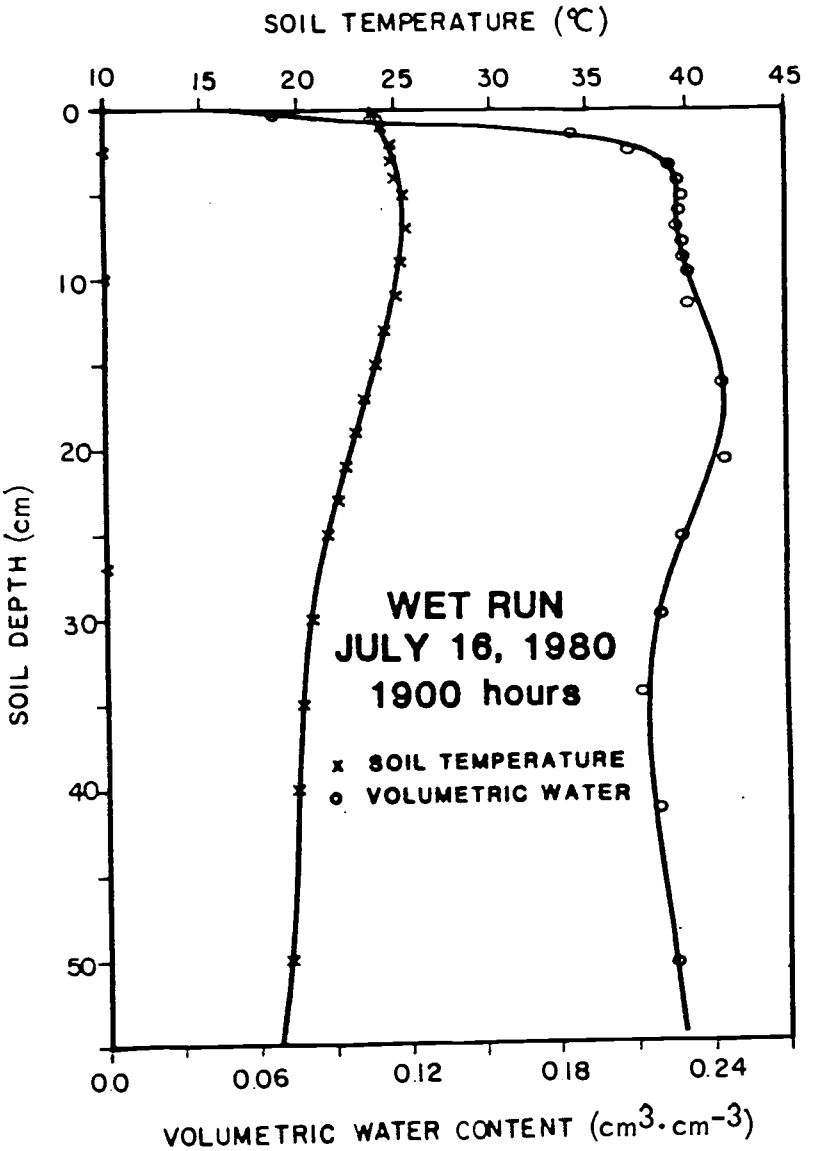

Figure 10. Soil temperature and volumetric water content distributions at 1900 hours on the wet treatment Walla Walla silt loam field plot.

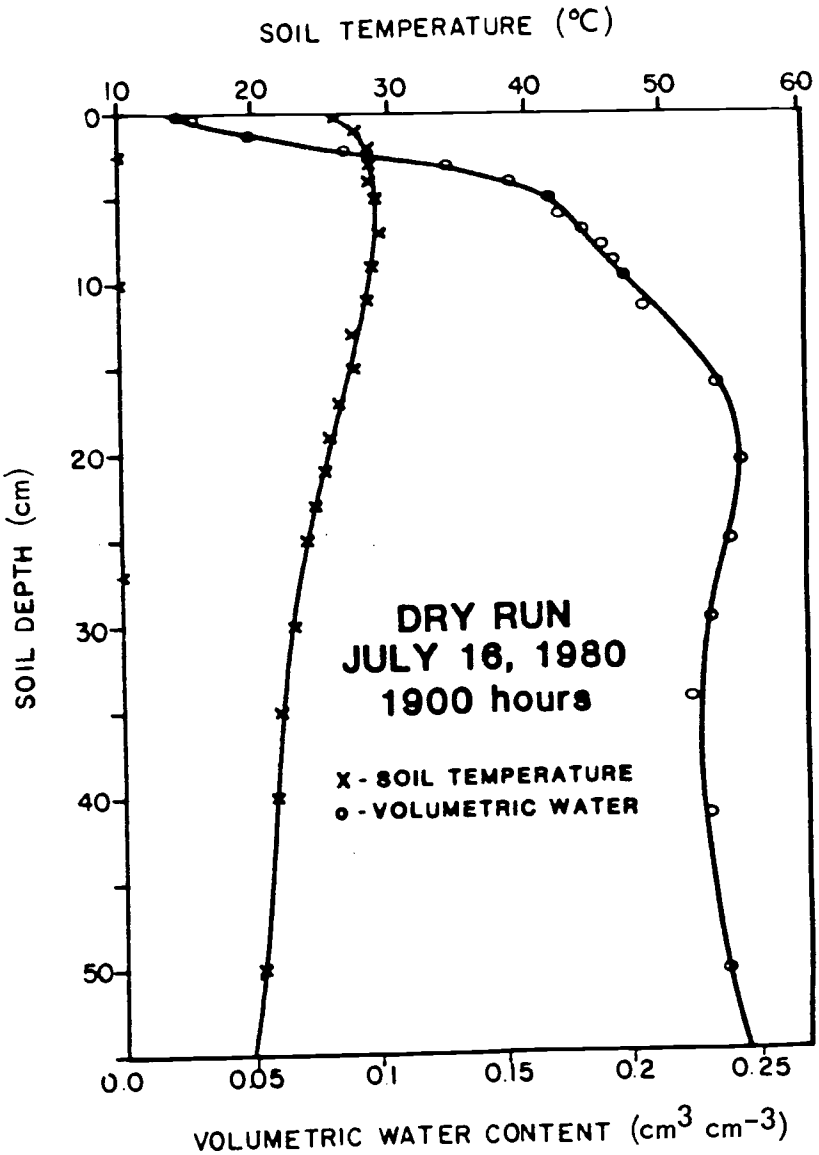

Figure 11. Soil temperature and volumetric water content distributions at 1900 hours on the dry treatment Walla Walla silt loam field plot.

Criteria by Kimball and Jackson (1975), indicate that liquid water flow at the null depth should be negligible. In the case of the wet treatment, liquid flow may have occurred (Table 3); however, it is doubtful that this flow carried substantial heat because of the near isothermal conditions (Fig. 10) at the depths of interest (5 to 30 cm). In the case of the dry treatment liquid flow in the 0- to 8-cm profile (the portion of the profile where outlying values occur) was negligible because of extremely small hydraulic conductivities (Figs. 5b and 11). However, even if substantial liquid flow were taking place, heat transport would be negligible because of near isothermal conditions (Fig. 11).

The possibility of latent heat transport in the top 8 cm of the dry plot along steep water-content gradients (Fig. 11) may account for the anomalous NARDTC's. At this time of the day it is possible that isothermal vapor-transport along vapor-pressure gradients plays the dominant transport role because large thermal gradients are non-existent. Further discussion of vapor transport will be deferred to later sections. Suffice it to say that the water and temperature regimens of the dry treatment favor latent-heat transport (Jackson, 1965; Cary, 1966) at the shallow null-point depths. To avoid erroneous NARDTC's shallow-depth null points should be used with caution. In this work a depth of 15 cm was selected as a cutoff criteria for null point selection. All NARDTC's that fell between 15 and 35 cm were considered reasonable values and used to obtain an average daily thermal conductivity at the 35-cm reference depth.

Kimball and Jackson (1975) acknowledge that some scatter will occur among the values (null-aligned reference depth conductivity)

Table 3. Measured water content change, predicted isothermal liquid flux and calculated vapor flux for soil slabs in the top 11 cm of soil.[1/]

Soil slab (cm)	Measured change (cm)	Isothermal liquid (cm)	Vapor (cm)
- - - - - - - - - - - - Wet treatment - - - - - - - - - - - - - - - - -			
0.25-1	-0.0861	-	-
1 -2	-0.0635	-	-
2 -3	-0.0411	-	-
3 -4	-0.0336	-0.2500	0.0014
4 -5	-0.0290	-0.1726	0.0006
5 -7	-0.0458	-0.0185	0.0008
7 -9	-0.0306	0.1084	0.0015
9 -11	-0.0192	0.0732	0.0015
- - - - - - - - - - - - Dry treatment - - - - - - - - - - - - - - - - -			
0.25-1	-0.0013	-	-
1 -2	-0.0006	-	-
2 -3	-0.0014	-	-
3 -4	0.0009	0.064	-0.0016
4 -5	0.0034	0.0083	0.0006
5 -7	0.0057	-0.0321	0.0031
7 -9	0.0053	0.0325	0.0025
9 -11	0.0064	0.0369	0.0029

[1/] A positive sign indicates a net gain during 24 hours.

obtained from the different profiles. In their error analysis, they found that, if the value of the thermal conductivity at 20 cm were off by 30%, only a 1% error would be introduced in the surface soil-heat-flux at midday and a 10% error when the temperature gradient at 20 cm was at its maximum (Equation [6]). To avoid the large error induced by temperature gradient one may be tempted to select a deep reference depth. If the reference depth is too deep however, the temperature change may be too small to be measured accurately. Clearly the null-alignment method requires caution in the selection of a reference depth and subsequent evaluation of null-aligned reference depth thermal conductivities for a particular soil and time of year (propagation of the daily temperature wave). When compared to other heat flux measurement procedures (Tanner, 1963; Kimball and Jackson, 1975) the constraints of the null alignment method were considered to be minor. Total soil heat flux, including the mechanisms of conduction, liquid water flow, and latent heat distillation, as calculated in this section is used as a standard of comparison for the theoretical heat flux method of Philip and de Vries as discussed in the next section.

Philip and de Vries Theoretical Heat Flux

Heat is transferred in soils mainly by conduction through solid particles, water, and air (listed in descending order of importance). Convective heat transfer may also occur when air pressure changes induce mass movement of soil air, or, as in wet soils, liquid water flow is taking place. A third major means of heat flux in soils occurs when a mixture of air pores and water films supports the transport of latent heat by water vapor diffusion. As water vapor molecules diffuse from

warm to cold and wet to dry regions latent heat transfer also modifies the thermal conductivity of the medium.

Soil water influences heat flow in a number of ways. As stated in Equation [8], water acts in a passive manner as a constituent of the soil heat capacity. Water also plays an active role in the transport of latent heat by water vapor diffusion and convective transport. Philip (1957) accounted for the total vertical soil heat flux, Gc, due to a water content gradient (isothermal heat flux) and a temperature gradient (thermal heat flux):

$$Gc_{ij} = -\lambda_{ij} \cdot (dT/dz)_{ij} - \rho l_{ij} \cdot L_{ij} \cdot D\theta v_{ij} \cdot (d\theta/dz)_{ij} \quad [9]$$

.... $(mcal/cm^2 \cdot sec)$

where λ = apparent thermal conductivity of the soil (mcal/cm·sec·C),

ρl = density of liquid water (g/cm^3),

L = latent heat of vaporization of water (mcal/g), and

$D\theta v$ = isothermal vapor diffusivity cm^2/sec.

The apparent thermal conductivity of the soil was calculated using the theory of de Vries (1963). de Vries used a method analogous to expressing the dielectric constant of a granular material in the volume fractions and physical properties of its constituents:

$$\lambda = \sum_{i=1}^{N} K_i \cdot X_i \cdot \lambda_i / \sum_{i=1}^{N} K_i \cdot X_i \quad .... \ (mcal/cm \cdot sec \cdot C) \quad [10]$$

where N = number of granule types,

K = is a ratio of the average temperature gradient in the granule to that in the continuous medium,

X = volume fraction of a granule type, and

λ = thermal conductivity of a granule type.

For use of the de Vries model, this soil was assumed to be composed of only three distinct components: volume fraction of water (Xw), solids (Xs), and gas filled pores (Xa), each of which has a thermal conductivity λw, λs, and λav, respectively. Water is considered as the continuous medium for all $\theta \geq 0.20$ cm^3/cm^3. Equation [10] is rewritten for this work as:

$$\lambda_{ij} = \frac{Xw_{ij}\lambda w_{ij}+Ks_{ij}Xs_{ij}\lambda s_{ij}+Ka_{ij}Xa_{ij}\lambda av_{ij}}{Xw_{ij}+Ks_{ij}Xs_{ij}+Ka_{ij}Xa_{ij}} \quad [11]$$

.... (mcal/cm•sec•C)

In moist soils temperature gradients cause moisture movement. Changing temperature fields cause moisture redistribution in both the liquid and vapor phases. Sensible and latent heat are transported when moisture redistributes, and this transport of latent and sensible heat will change the temperature distribution. A quantitative treatment of the combined heat and water flow requires the solution of two differential equations with soil temperature and water content as two dependent variables. Krischer and Rohnalter (1940) were the first to propose a simple treatment to approximate the influence of moisture movement on the heat transfer in soils. This simplified theory neglected the transport of sensible heat due to moisture movement. Philip and de Vries (1957) and de Vries (1958) further modified this theory for soil air not saturated with water vapor. In Equation [11] the variable λav accounts for the transport of latent heat in gas-filled pores. Water vapor diffusion occurs under the influence of temperature gradients that give rise to vapor pressure gradients. Because the vapor flux due to temperature differences is nearly proportional to the temperature gradient across the gas filled pore the transport of heat can be viewed

as an apparent increase in heat conduction. This apparent increase is that due to heat conduction in dry air, λa, plus that due to vapor movement, λv, as written in Equation [12]:

$$\lambda av_{ij} = \lambda a_{ij} + \lambda v_{ij} \text{ .... (mcal/cm·sec·C)} \quad [12]$$

The thermal conductivity of dry air was expressed as an empircal function of soil temperature (Kimball et al., 1976):

$$\lambda a_{ij} = 0.0566 + 0.000153\ T_{ij} \text{ .... (mcal/cm·sec·C)} \quad [13]$$

The Krischer and Rohnalter expression accounts for vapor movement when air in the soil pores is saturated with water vapor. Philip and de Vries found this expression to be proportional to the relative humidity of the soil air for conditions less than saturation:

$$\lambda v_{ij} = [hLDa\gamma(d\rho o/dT)]_{ij} \text{.... (mcal/cm·sec·C)} \quad [14]$$

where h = fractional relative humidity of the soil air,

L = latent heat of vaporization of water (mcal/g),

Da = diffusion coefficient for water vapor in air (cm^2/sec),

γ = mass flow factor which accounts for the mass movement of soil air due to the unequal diffusion rate of air and water vapor molecules, and

$d\rho o/dT$ = saturated water vapor density gradient ($g/cm^3 \cdot C$).

Relative humidity was calculated using an empirical equation developed by Fink and Jackson (1973):

$$h_{ij} = [1 + (\theta_{ij}/a\rho b_{ij})^{1/B}]^{-1/C} \text{ .... (unitless)} \quad [15]$$

where a = 0.03579 cm^3/g, B = -0.241, C = 2.13 for sorption, or a = 0.04328 cm^3/g, B = -0.224, C = 2.62 for desorption of water vapor from Adelanto loam. The choice of a drying or wetting limb of the daily hysteresis loop to compute h was aided by an inspection of $\Delta\theta/\Delta t$. The

soil layer was considered to be desorbing when $\Delta\theta/\Delta t < 0$, otherwise adsorption was assumed.

Latent heat of vaporization of water was calculated as a linear function of soil temperature (Kimball et al., 1976):

$$L_{ij} = 10^3(595.9 - 0.548\ T_{ij}) \ldots\ (\text{mcal/g}) \qquad [16]$$

The diffusion coefficient for water vapor in air as a function of soil temperature was computed (Dorsey, 1940) as:

$$Da_{ij} = 0.229\ [(T_{ij}+273)/273]^{1.75} \ldots\ (\text{cm}^2/\text{sec}) \qquad [17]$$

The mass flow factor, γ, from Van Bavel (1952) as written by Jury (1973) takes into account the movement of the air mass in binary diffusion:

$$\gamma = P/(P-Pv) \ldots\ (\text{unitless}) \qquad [18]$$

Where P = total gas pressure of the soil air taken as the barometric pressure at the research site (980 mbar), and

Pv = partial vapor pressure of water in the soil air.

A convenient form of Equation [18] is obtained by using the ideal gas law to find the partial vapor pressure of water in the soil air in terms of the saturated water vapor density and relative humidity. The ideal gas law is written:

$$Pv = nR(T+273)/V \ldots\ (\text{mbar}) \qquad [19]$$

where n = moles of water (g/18.016 g/mole),

R = gas constant (83144 mbar·cm^3/mole·K)

V = volume of gas (cm^3).

Then by using the definition of n and the dimensions of density (mass/volume) Equation [19] can be rewritten in terms of the saturated water vapor density, ρo, and relative soil air humidity:

$$Pv = R(T+273)\rho oh/18.016 \ldots\ (\text{mbar}) \qquad [20]$$

Equation [20] is then substituted into Equation [18] to obtain:

$$\gamma_{ij} = P/[P-h_{ij}\rho o_{ij}R(T_{ij}+273)/18.016] \ldots . \text{ (unitless)} \quad [21]$$

The saturated water vapor density is computed as a function of temperature using the relation as written by Kimball et al. (1976):

$$\rho o_{ij} = 10^{-6} \exp[19.819 - 4975.9/(T_{ij}+273)] \ldots . (g/cm^3) \quad [22]$$

and finally $d\rho o/dT$ from:

$$\frac{d\rho o}{dT} = 4975.9\ \rho o_{ij}/(T_{ij}+273)^2 \ldots . (g/cm^3 \cdot C) \quad [23]$$

A reconciliation of the equations used by de Vries (1963), de Vries (1975), Kimball et al. (1976) and those of this paper to calculate thermal conductivity due to vapor movement (Equation [14]) is shown in Appendix 2. There is a general agreement among the methods except de Vries (1963, Equation 7.12). This equation [7.12] for the diffusion of water vapor in air as proposed by Krischer and Rohnalter (1940) underestimates Da by a factor of ten as compared to the methods of Dorsey (1940) as used by Kimball et al. (1976), de Vries (1975), and List (1958).

Thermal conductivity of the solid soil components in Equation [11] was determined to be 9.98 mcal/cm•sec•C. It is a thermal conductivity weighted according to the percentage weight composition of quartz, non-quartz mineral, and organic matter in the bulk soil (Table 1).

Thermal conductivity of water is expressed as an empirical function of temperature (Kimball et al., 1976):

$$\lambda w_{ij} = 1.32 + 5.59 \times 10^{-3}\ T_{ij} - 2.63 \times 10^{-5}(T_{ij})^2 \quad [24]$$

$$\ldots . \text{ (mcal/cm•sec•C)}$$

The volume fraction of water is calculated using Equation [2], and the volume fraction of air is:

$$Xa_{ij} = (1 - \rho b_i/2.657) - \theta_{ij} \quad \ldots\ \text{(unitless)} \qquad [25]$$

Solids fraction is calculated as:

$$Xs_{ij} = 1 - (1 - \rho b_i/2.657) \quad \ldots\ \text{(unitless)} \qquad [26]$$

In Equation [11] K represents the ratio of the space average of the temperature gradient in the soil solids, Ks, (or air, Ka) to that of the temperature gradient in the continuous medium. In this work water is the continuous medium for all $0.20 \leq \theta_{ij} \leq (1 - \rho b_i/2.657)$. K values were calculated from:

$$K_m = \frac{1}{3}\sum_{j=1}^{3}\left[1 + \left(\frac{\lambda m}{\lambda c} - 1\right) g_{mj}\right]^{-1} \quad \ldots\ \text{(unitless)} \qquad [27]$$

where the subscripts m and c denote the "medium" conductivity (solids or air) and the continuous medium (water), respectively. The g_{mj} are shape (depolarization) factors which account for the shape of granules and their orientations with respect to the three axes of physical space. If the soil is considered to be composed of spheroids (de Vries, 1963) then the sum over j of three g_m is unity and Equation [27] reduces to:

$$Ks_{ij} = \frac{2}{3\left[1+\left(\frac{\lambda s}{\lambda w_{ij}} - 1\right)(g_s)\right]} + \frac{1}{3\left[1+\left(\frac{\lambda s}{\lambda w_{ij}} - 1\right)(1-2gs)\right]} \qquad [28]$$

$$\ldots\ \text{(unitless)}$$

for soil solids having a single shape factor of gs = 0.144 (Kimball et al., 1976). For air, Ks in Equation [28] becomes Ka, λav is substituted for λs and ga for gs. Values of ga were taken from Wierenga et al. (1969) wherein ga was made to decrease linearly from 0.333 in water-saturated soil to 0.105 at a soil water content of 0.20. Below

θ = 0.20, ga was assumed to decrease linearly to a value of 0.015 at oven-dryness. For $\theta \geq 0.20$, ga is represented by:

$$ga = 0.333 - \frac{0.228\ Xa_{ij}}{(1-\rho b_i/2.657)-0.20} \quad \ldots. \text{ (unitless)} \qquad [29]$$

The foregoing discussion of Equations [27] through [29] departs in two respects from the de Vries (1963) method to estimate thermal conductivity of granular material. First, the critical water content used here is 0.20 cm^3/cm^3 and second, the air shape factor is smaller than that proposed by de Vries.

de Vries (1963) indicates that at low moisture contents it is not permissible to consider water as the continuous medium. Rather, a graphical interpolation should be used between Xw=0 and some critical Xw. de Vries suggests this critical value (θ_c) be about 0.03 for coarse-textured soils and 0.05 to 0.10 for fine-textured soils. Water is generally considered the continuous medium in the range where the apparent conductivity of the air-filled pores is equal to $\lambda a + \lambda v^s$, or where the relative humidity fraction is considered 1.0. Kimball et al. (1976) used the Fink-Jackson formula for relative humidity and determined, for an Avondale loam, that soil humidity departs from 1.0 significantly at about the wilting point where θ=0.15 cm^3/cm^3. Wierenga et al. (1969) considered the air in soil pores to be water saturated above 0.20 cm^3cm^{-3} for a Yolo silt loam, however no explanation was offered for this critical value. Sepaskhah (1974) and Sepaskhah and Boersma (1979) determined critical water values by trial and error. Critical water values were chosen at the points where the apparent thermal conductivity declined sharply as soil water content decreased. For Quincy loamy sand, Cloquato loam, and Chehalis silt loam this

critical water content was determined as 0.25 cm^3/cm^3 at 25°C. Hadas (1977) does not indicate a critical water content and refers the reader to de Vries (1963). Cochran et al. (1967) assumed a decrease in λ_v at 0.15 mcal/sec·cm·C and the corresponding θ = 0.12 cm^3/cm^3 was used as the critical water content for a pumice soil. This decrease is not well defined in the figure referred to by Cochran et al. (1967). For the Walla Walla silt loam a sharp decrease in λ_v was not obvious in the range of water content from field capacity to the wilting point. The criteria for critical water content determination for this work followed the methods of Kimball et al. (1976) and relative humidity was found to depart from 1.0 at about θ = 0.20 cm^3/cm^3.

The second major departure from the de Vries (1963) theory was made in the selection of an air shape versus water content curve. Kimball et al. (1976) presents an in-depth analysis of various air shape factors and the result on calculated heat flux. In an attempt to find the best air shape curve for their soil, an iteration procedure was used to match theoretical fluxes to measured fluxes. Both positive and negative air shape factors indicated that the air shape factor concept is physically unrealistic or meaningless for the Avondale loam. Such an analysis was not attempted in this study. Rather a compromise position was taken in the selection of a ga curve. The curve selected by Wierenga et al. (1969) lies below that proposed by de Vries (1963) and above the best fit curve of Kimball et al. (1976). A smaller selected ga will reduce ka and λ and ultimately the calculated soil heat flux.

When water was no longer taken to be the continuous medium (Xw < 0.20 cm^3/cm^3) apparent soil thermal conductivity was calculated using

a linear interpolation between Xw = 0 and Xw = 0.20 cm^3/cm^3. Thermal conductivity at Xw = 0.20 cm^3/cm^3 was obtained using Equations [11, 27, 28, 29]. At Xw = 0 dry air was used as the continuous medium and K_s' was calculated as:

$$K'_{s_{ij}} = \frac{2}{3[1+(\frac{\lambda s}{\lambda a_{ij}} 1)gs]} + \frac{1}{3[1+(\frac{\lambda s}{\lambda a_{ij}} - 1)(1-2gs)]} \quad [30]$$

.... (unitless)

de Vries corrected his thermal conductivities at Xw = 0 by a factor of 1.25. This was also used to obtain λ at Xw = 0:

$$\lambda(Xw=0) = \frac{Xa_{ij}\lambda a_{ij}+K's_{ij}\ Xs_{ij}\lambda s}{Xa_{ij}+ K's_{ij}Xs_{ij}} \cdot 1.25 \quad .... \text{ (mcal/cm·sec·C)} \quad [31]$$

Interpolated λ for $0 < Xw < 0.2$ was found as:

$$\lambda = [\frac{\lambda(X_w=0.2)-\lambda(X_w=0)}{0.20}]\cdot X_w+\lambda(X_w=0) \quad .... \text{ (mcal/cm·sec·C)} \quad [32]$$

where Xw, in this case, is the desired interpolation water content. An example of apparent soil thermal conductivity for θc = 0.10 and 0.20 cm^3/cm^3 is shown in Fig. (12). Dashed lines indicate the interpolation values for $0 < Xw < \theta c$. Obviously, the selection of a critical water content greatly influences the interpolation values when a linear interpolation is used as suggested by de Vries (1963).

To isolate conduction heat flux from the total, K_s is calculated as in Equation [28]. For dry air K_a' is calculated as in Equation [28] by substituting K_a' for K_s, λa for λs, and ga for gs. This procedure produces a calculated Ka value using thermal conductivity of dry air, λa, with no vapor flux enhancement. Thermal conductivity of conduction only, λc, is then recalculated using Equation [11] and substituting λa for λav and K_a' for Ka. Conduction heat flux, G_o, is obtained as:

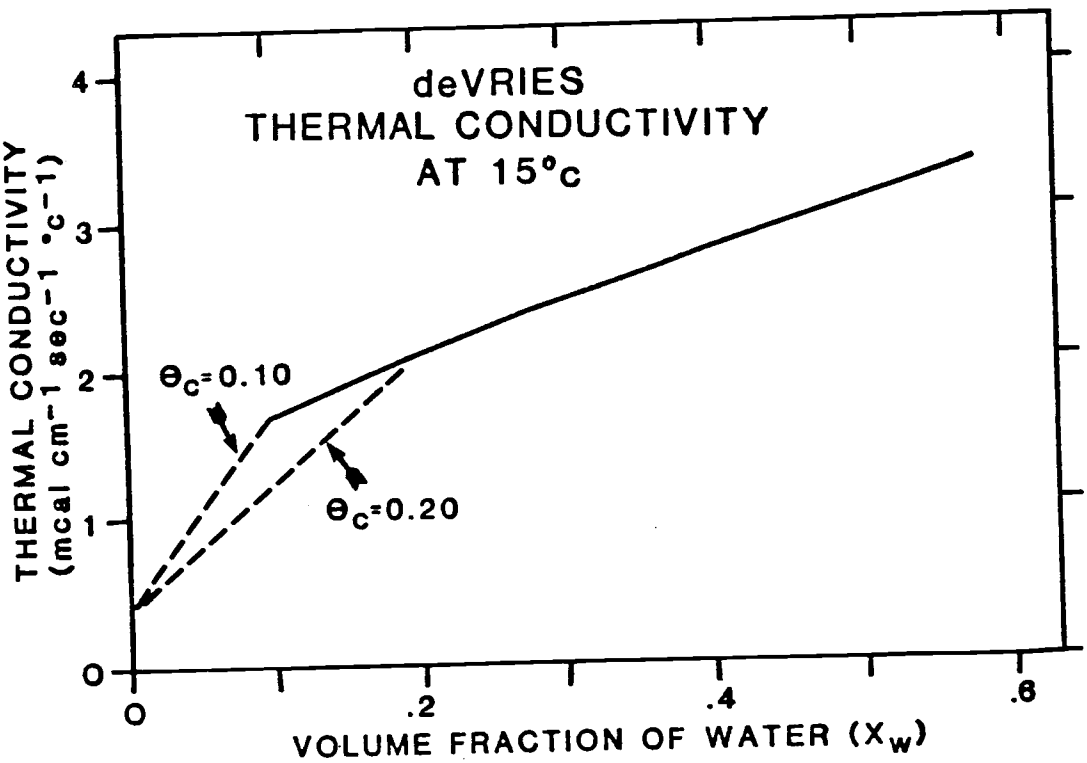

Figure 12. Graphical interpolation (dashed line) of de Vries theoretical thermal conductivity between Xw = 0 and critical water contents of 0.10 and 0.20 cm^3/cm^3.

$$Go_{ij} = \lambda c_{ij} \left(\frac{dT}{dz}\right)_{ij} \text{ .... } (mcal/cm^2 \cdot sec) \quad [33]$$

The vapor flux, Gv, component of the total calculated heat flux is then found as:

$$Gv_{ij} = Gc_{ij} - Go_{ij} \text{ .... } (mcal/cm^2 \cdot sec) \quad [34]$$

where Gc is the total calculated heat flux as written in Equation [9].

In Equation [9] liquid water density, $\rho\ell$, in the 4 to 40°C temperature range was fitted to a 3rd degree polynomial:

$$\rho\ell_{ij} = 0.999837 + 6.203 \times 10^{-5} T_{ij} - 7.887 \times 10^{-6} (T_{ij})^2 + 3.991 \times 10^{-8} (T_{ij})^3 \text{ .... } (g/cm^3) \quad [35]$$

The isothermal vapor diffusivity (Philip and de Vries, 1957) is expressed as:

$$D\theta v_{ij} = [Da\alpha\gamma(\rho o/\rho\ell)(dh/d\theta)]_{ij} \text{ .... } (cm^2/sec) \quad [36]$$

where α is a dimensionless geometry factor. Vapor diffusion in soil is less than in air because of reduced cross section area and tortuous path length. Currie (1960, 1961) showed that the geometry factor was not a direct and unique function of gas-filled porosity. Rather in a soil-water system the diffusion coefficient depended upon the site of drainage, whether from the large interaggregate pore space or smaller pores within aggregates. Fractional reduction in the diffusion coefficient for a gas insoluble in water follows Currie (1960, 1961):

$$\alpha_{ij} = D/D_o = (D/Ds)(Ds/Do) \text{ .... } (unitless) \quad [37]$$

where: D = the diffusion coefficient for an insoluble gas in moist soil,

D_o = the diffusion coefficient for an insoluble gas in air, and

D_s = the diffusion coefficient for an insoluble gas in dry soil.

Ratios of Ds/Do versus the total porosity fraction, ε, for Barnfield 80,

Highfield and Woburn soil crumbs (Currie, 1960), extended to Ds/Do = 0 when ε = 0 and Ds/Do = 1 when ε = 1, was approximated by a third degree polynomial shown in Fig. 13. Ratios of the gas-filled porosity-fraction to the total porosity-fraction $\varepsilon g/\varepsilon$ versus the ratio of D/Ds for Barnfield 80 soil crumbs (Currie, 1961), extended to include Ds/Do = 0 when ε = 0 and Ds/Do = 1 when ε = 1, and fitted to a cubic spline are shown in Fig. 14. The relation between D/Ds and $\varepsilon g/\varepsilon$ when ε is decreased by increasing water content was investigated by Currie (1961) for a wide range of porous materials. Currie found that his experimental relationship between D/Ds and $\varepsilon g/\varepsilon$ for Barnfield 80 soil crumbs varied only modestly with other natural soils. From the smooth curves in Fig. 13 and 14 values of

$$(Ds/Do)_{ij} = f(\varepsilon)$$

and

$$(D/Ds)_{ij} = f(\frac{\varepsilon g}{\varepsilon})_{ij}$$

were obtained for the appropriate bulk density and volumetric water fractions and ultimately α in Equation [37]. The relative humidity gradient expressed in terms of θ is:

$$(dh/d\theta)_{ij} = [-h_{ij}^{1+cB}(1-h_{ij}^{c})^{1-B}]/(acB\rho b_{ij}) \quad \ldots\ \text{(unitless)} \quad [38]$$

Thus, measurements of bulk density, soil water content, temperature and mineral composition, and the defined coefficients were used to calculate total soil heat flux using Equation [9].

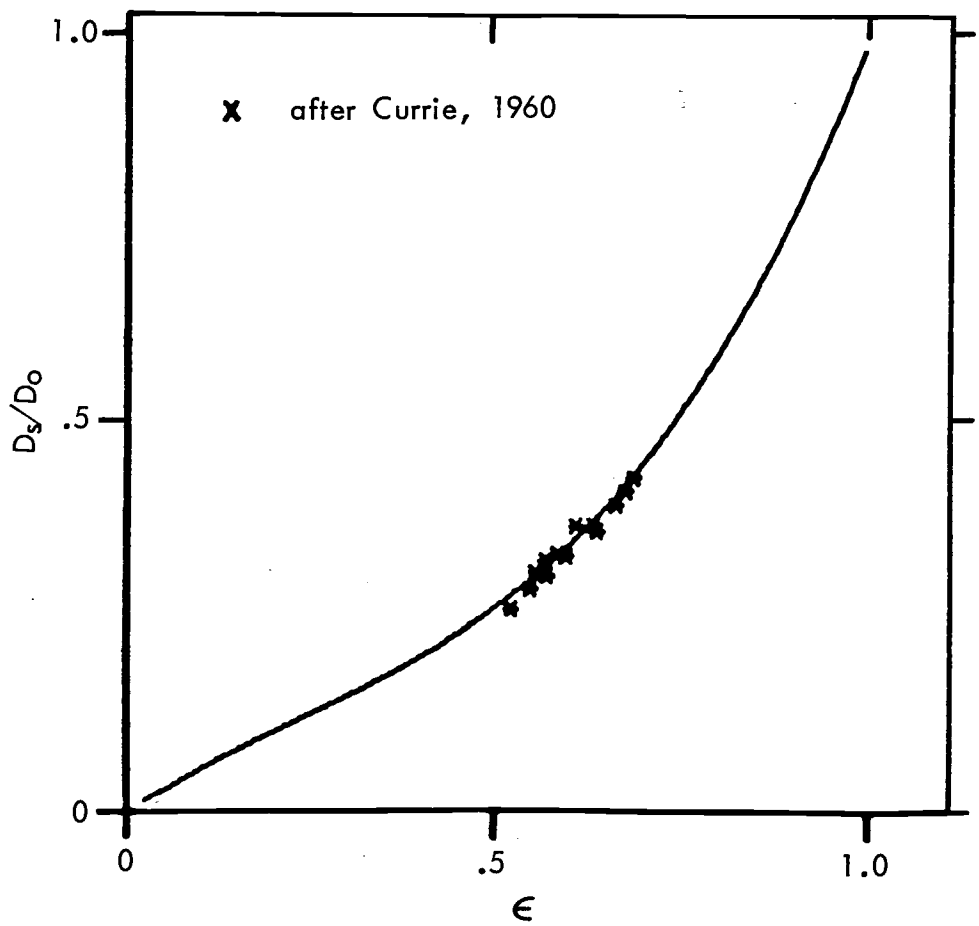

Figure 13. Total porosity fraction (ϵ) versus the ratios of the diffusion coefficient for an insoluble gas in dry soils (Ds) to that of an insoluble gas in air (Do).

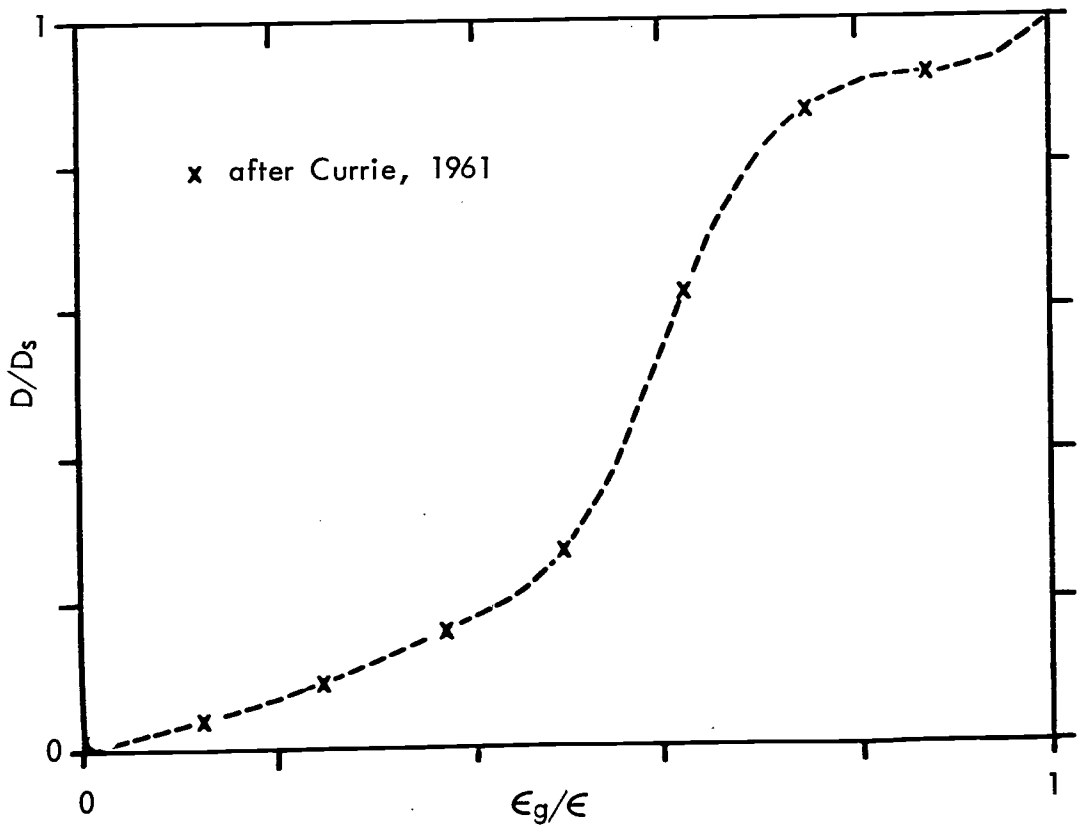

Figure 14. Ratios of the gas-filled porosity fraction (εg) to the total porosity-fraction (ε) versus the ratios of the diffusion coefficient for an insoluble gas in moist soil (D) to that of an insoluble gas in dry soil.

RESULTS AND DISCUSSION

Temperature Measurements

The dry soil treatment or plot was stubble covered while the wet soil plot was bare. This comparison is unlike the usual field situation in which stubble covered soils are generally wetter than adjacent bare soils. The stubble covered plot generally exhibited higher day and night soil temperatures throughout the top 35 cm of soil than the bare-surfaced plot (Figs. 1 and 2). At 0.25 cm the maximum and minimum soil temperatures were 14°C and 2.5°C warmer in the stubble covered dry soil than in the bare surfaced wet plot. Midday thermal gradients in the upper 3 cm of the bare plot were generally 2/3 as great as those in the stubble covered plot. Typically one would expect surface residue cover to depress soil temperatures by (i) insulating the soil surface and (ii) reflecting a greater fraction of solar radiation back to the atmosphere (van Wijk et al., 1959). The reflectivity of the bare soil and weathered crop residues at this location (Fig. 15) indicates that the bare soil surface reflected a higher percentage of the incident shortwave radiation than the weathered straw. These characteristics of the shortwave radiation budget and partitioning of energy both impart markedly different daytime soil thermal responses.

Convection is the principal means of transporting surplus energy away from a surface during the daytime. The relative importance of sensible (energy used to heat the air) versus latent heat of evaporation is mainly governed by the availability of water for evaporation (Oke, 1978). Because the bare surfaced plot was irrigated, the soil water content near the surface was substantially greater than the

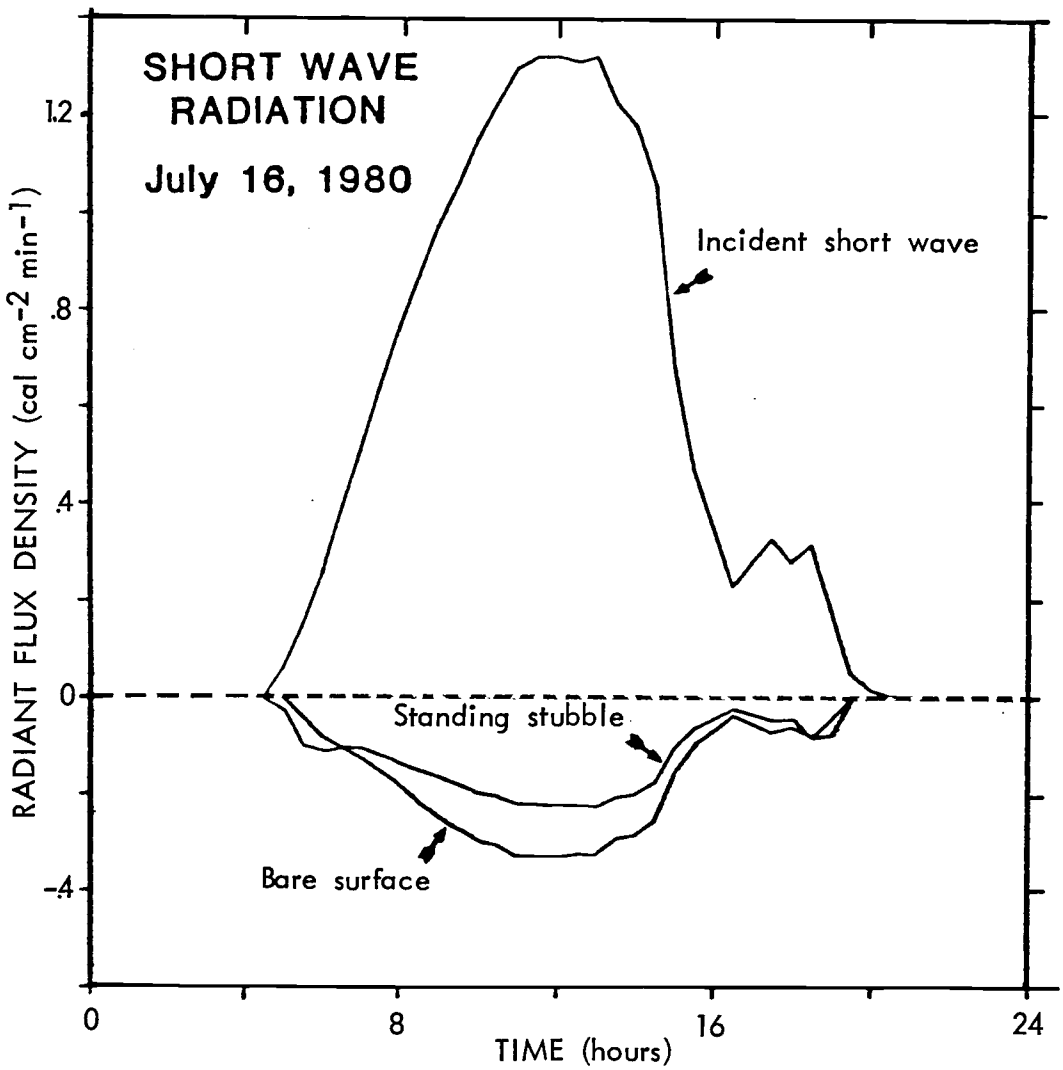

Figure 15. Short-wave radiation budget over the wet (bare) surface) and dry (stubble-covered) field plots.

straw covered dry plot (Figs. 4a, 4b, 10 and 11). Measured water content changes in the soil at 0.25 to 1 cm (Figs. 4a and 4b) and air temperature at 15 cm (Fig. 16) approximately indicate the partitioning of energy on the two plots. The bare surfaced plot partitioned 66% more energy into latent heat and 20% less into heating the air than the stubble covered plot. Thermal responses of the soil are directly proportional to the ability to transmit heat, λ, but inversely proportional to the amount of heat, H, required to effect a temperature change. These relationships are stated as $K_S = \lambda/H$ where the soil thermal diffusivity, K_S, is a measure of the time required for temperature changes to travel within the soil. The bare surfaced plot, with relatively high water contents near the surface, effectively slowed the propagation of heat into the soil and buffered against extreme soil temperatures with both large heat capacities and the partitioning of energy into latent heat.

On both plots spatial variability between the duplicate temperature sensors was greater than the temporal variability. Furthermore it appears that most of the calculated temporal variability was a reflection of the spatial differences between the temperature probes. Spatial standard deviations of duplicate temperature sensors at 1-cm were 0.51 and 1.69 and at 35-cm 0.37 and 0.20°C for the bare and stubble covered plots, respectively. Temporal standard deviations were calculated using the measured mean temperatures and the Fourier-smoothed temperatures. These standard deviations at 1-cm were 0.19 and 0.23 and at 35-cm 0.06 and 0.08°C for the bare and stubble covered plots, respectively. Because the bare surfaced plot was irrigated soil temperature regimes are unlike the expected field situation.

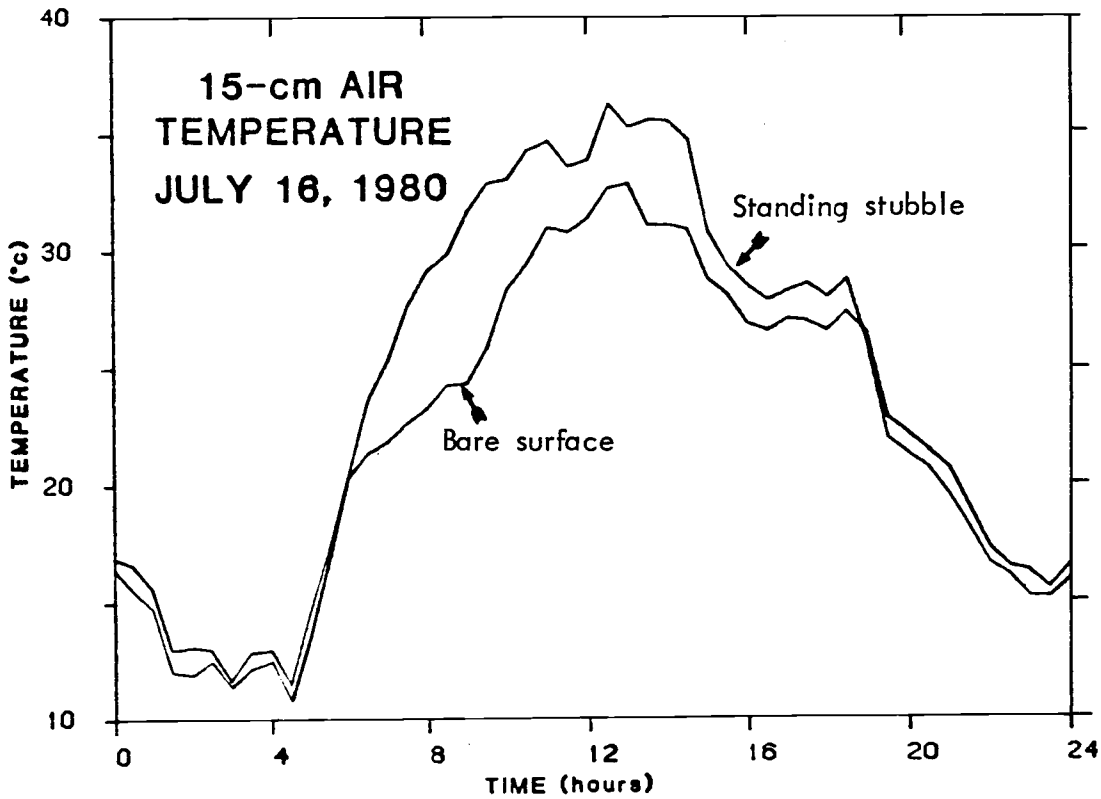

Figure 16. 15 cm air temperature over the wet (bare surface) and dry (standing stubble) Walla Walla silt loam field plots.

However, this abnormality does not preclude a satisfactory Philip-de Vries heat flux calculation.

Soil Water Measurements and Hydraulic Properties

During the 24-hour measured period the irrigated-bare surfaced plot lost nearly 1 mm of water to evaporation in the 0.25- to 1-cm layer. This compares to a loss of 0.01 mm, or essentially no measurable change, on the stubble covered dry plot. Diurnal volumetric water at 0.25, 1, 2, 3, 4 and 5 cm for the wet and dry plots is shown in Figs. 4a and 4b, respectively. These field measured values represent the total water profile change in response to thermal and isothermal liquid and vapor fluxes.

To make a reasonable interpretation of calculated vapor heat fluxes, on the wet plot, the possibility of liquid flux could not be ignored. On this plot an attempt was made to isolate isothermal liquid water flux. For the dry soil conditions found on the dry plot extremely low hydraulic conductivities precluded significant liquid flux. Vapor flux was therefore assumed to be the dominant mechanism for water movement. Isothermal liquid water flux at a soil slab boundary was computed using Equation [4] and slab storage as in Equation [5]. Generally the results (Table 3) indicate a tenfold overestimation of Darcy liquid flux on both the wet and dry plot.

Although additional field measurements will be necessary to determine the cause of overestimating isothermal liquid flow, it is likely that hydraulic properties were not uniform over depth as assumed. The water release curve and the hydraulic conductivity function both may be nonhomogeneous over depth. The water release curve for this

soil, especially in the tensiometric range, may be best represented by a series of curves rather than a composite of samples taken from the top 30 cm (Fig. 5a). The presence of three distinct structural soil layers support this viewpoint: 1) a tillage layer at 0 to 19-cm that is worked to a fairly uniform depth each year, 2) a pressure pan at 19 to 26-cm characterized by high bulk density (Fig. 3), and 3) from 26 cm to depths of at least 2 m the soil is uniform with little change in dry bulk density or hydraulic properties.

There is also strong evidence to support a profile dependent hydraulic conductivity function. Figure 5b shows field measured conductivities at 30 cm for water contents in the 0.2- to 0.3-cm^3/cm^3 range. Calculated hydraulic conductivities based on the Marshall pore interaction model (Green and Corey, 1971) using a matching saturated conductivity of 2 cm/day (measured at 15 cm) are shown as a continuous curve. Calculated and field measured curves diverge with increasing intermediate water contents (Fig. 5b) and converge at about 0.2 cm^3/cm^3.

In the pressure pan a low saturated hydraulic conductivity of 2 cm/day is not uncommon (Pikul, unpublished). Because this low conductivity was used, Fig. 5b may best represent the conductivities of the 19 to 26-cm layer rather than the higher conductivity tillage layer. However, results in Table 3 for the 0 to 11-cm tillage zone indicate an overestimation of Darcy liquid flux despite the numerically low values of hydraulic conductivity used in Equation [4]. The water release curve (Fig. 5a) used to determine hydraulic heads and calculated hydraulic conductivity may need further field evaluation especially in

the 0.05 to 0.25 cm^3/cm^3 range. This water content range represents the bulk of the water flux calculations on both plots, however the sparse number of field measurements do not adequately define the curve in this region. A reduction of the slope ($dH/d\theta$) throughout this range would reduce the water fluxes calculated by Equation [4]. More field verification is necessary before the water release and hydraulic conductivity functions of Figs. 5a and 5b can be used with confidence to predict daily Darcy water fluxes.

On both plots the spatial variability of individual soil water content samples was compared to temporal variability using methods similar to the analysis of soil temperature variability. As with the soil temperature analysis it appeared that most of the calculated temporal variability was largely a reflection of spatial differences between composited individual soil samples. Spatial standard deviations of individual soil samples at 0.5-cm and 11.5-cm was 0.022 and 0.0052 cm^3/cm^3, respectively. Temporal standard deviations were calculated using the measured mean water content and the cubic-spline smoothed estimates. These standard deviations at 0.5-cm were 0.0096 and 0.0056 and at 11.5-cm 0.0092 and 0.004 cm^3/cm^3 for the wet and dry plots, respectively.

The field procedure to obtain gravimetric water changes reliably characterizes field water conditions over time and depth. Measured water changes on both plots provide an adequate data base for both heat flux methods. Although Darcy liquid fluxes were not accurately described this does not distract from the independent comparisons of soil heat flux methods.

Heat Flux

Calculated total soil heat flux by the methods of de Vries overestimated measured heat flux for most all times of day and at all depths to 35 cm. Measured and calculated daily total heat flux for 2, 5, 11, 17 and 35 cm are shown in Figs. 17a and 17b for the wet and dry soil treatments respectively. Not shown are comparisons of heat fluxes at 0.25 and 1.0 cm depths. Calculated fluxes at midday, corresponding to maximum soil temperature gradients, for these two shallow depths overestimated the null-alignment fluxes by a factor of four. Inaccurate measurements of soil temperature gradients at these shallow depths may have contributed to this fourfold overestimation of heat flux. A comparison of total net daily calculated and measured heat flux for all depths is shown in Table 4. The complete Philip-de Vries theory generally predicted net daily heat flux better for wet soil conditions rather than dry conditions. At seedzone depths predicted heat flux on the wet plot was about 10% greater than measured values as compared to nearly a 40% overestimation on the dry plot. At 35 cm both the wet and dry plot overestimate measured heat flux by about 25%.

The measured heat flux was tested for its sensitivity to account for heat storage in thin soil layers. In Figs. 18a and 18b measured and calculated soil heat flux at 5 and 17 cm, for the wet and dry plots, is plotted against temperature gradient. The slope of these plots is the thermal conductivity of the soil. Because dT/dz is not a functional component of Equation [7], this test checks performance of the null-alignment method for determining heat flux.

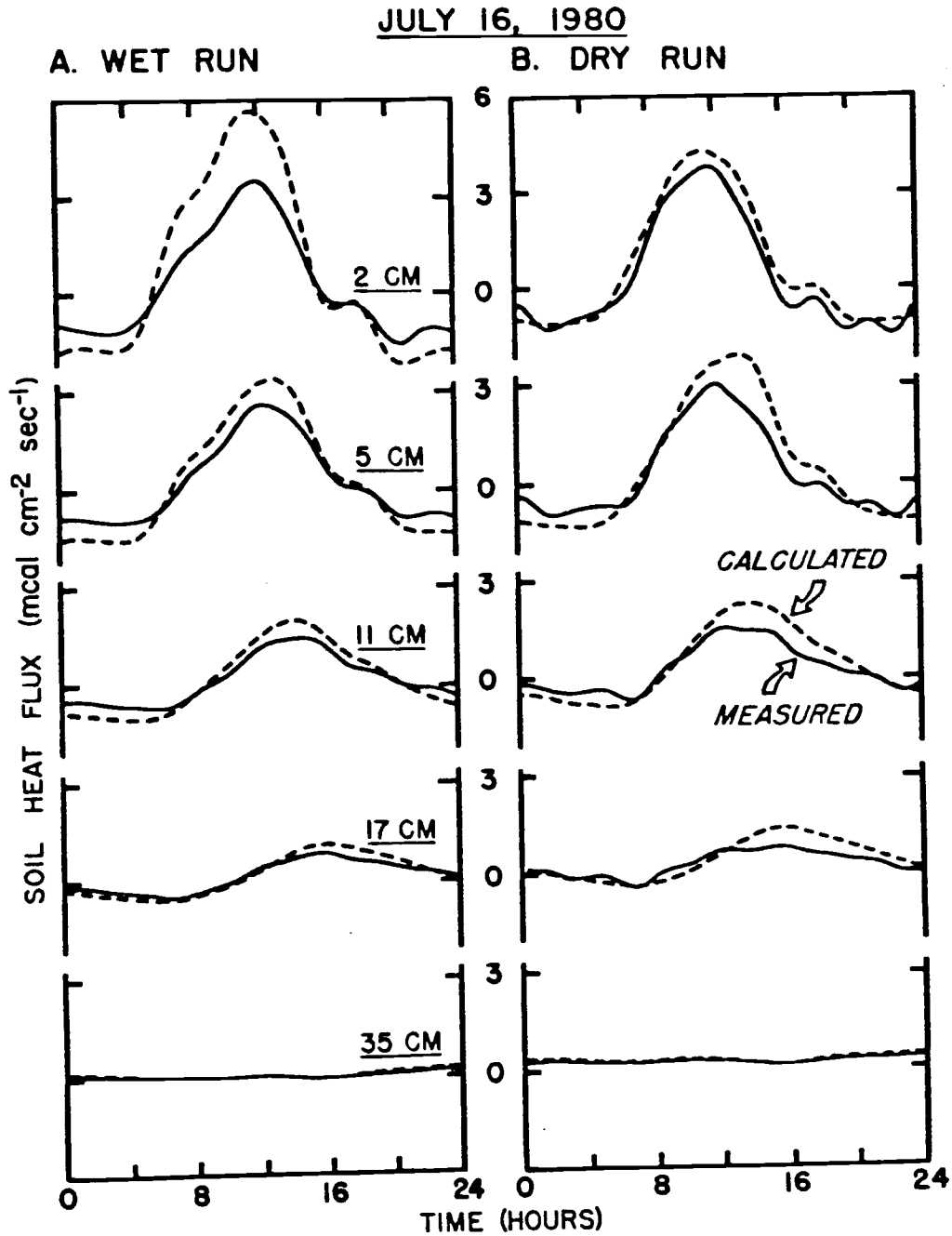

Figure 17. Diurnal measured and calculated soil heat flux at 2, 5, 11, 17, and 35 cm on the wet (A) and dry (B) Walla Walla silt loam.

Table 4. Average net daily soil heat flux calculated by the methods of Philip-de Vries and measured by the null-alignment method.

Depth	Measured	Conduction[1]	Conduction[2] error	Total[3]	Total[4] error	Measured	Conduction[1]	Conduction[2] error	Total[3]	Total[4] error
	-Net Daily Soil Heat Flux (cal/cm^2·day)-									
	Dry treatment					Wet treatment				
0.25	21.72	164.6	0.86	211.59	0.90	22.32	156.49	0.75	210.53	0.89
1.0	21.52	115.49	0.81	147.92	0.85	21.13	187.79	0.89	253.91	0.92
2.0	21.23	35.46	0.4	48.03	0.56	19.95	39.13	0.49	52.81	0.62
3.0	20.99	22.36	0.06	32.66	0.36	18.96	15.94	-0.19	21.78	0.13
4.0	20.84	24.93	0.16	36.11	0.42	18.05	15.93	-0.13	20.97	0.14
5.0	20.77	25.64	0.19	35.55	0.43	17.24	14.89	-0.16	19.61	0.12
7.0	20.7	25.02	0.17	34.24	0.4	15.76	12.92	-0.22	17.17	0.08
9.0	20.64	24.91	0.17	32.78	0.37	14.5	12.27	-0.18	15.71	0.08
11.0	20.59	25.78	0.2	32.11	0.36	13.4	12.08	-0.11	14.71	0.09
13.0	20.56	26.18	0.21	31.83	0.35	12.31	12.06	-0.02	14.17	0.13
15.0	20.51	27.86	0.26	32.74	0.37	11.31	12.06	0.06	13.84	0.18
17.0	20.43	29.07	0.30	33.43	0.39	10.39	11.97	0.13	13.54	0.23
19.0	20.34	29.53	0.31	33.52	0.39	9.56	11.66	0.18	13.1	0.27
21.0	20.19	29.2	0.31	32.97	0.39	8.82	11.15	0.21	12.51	0.29
23.0	19.94	28.28	0.29	31.88	0.37	8.18	10.51	0.22	11.81	0.31
25.0	19.64	26.94	0.27	30.43	0.35	7.67	9.81	0.22	11.07	0.31
30.0	18.85	23.12	0.18	26.39	0.29	6.85	8.26	0.17	9.46	0.28
35.0	18.33	20.47	0.10	23.54	0.22	6.54	7.52	0.13	8.7	0.25

[1] Pure conduction heat flux as calculated by Philip-de Vries theory Eq. [33].
[2] Conduction overestimates measured flux by 1 - (measured/conduction). Negative sign indicates underestimation.
[3] Total Philip-de Vries heat flux theory Eq. [9]. [4] Total overestimates measured flux by 1 - (measured/total).

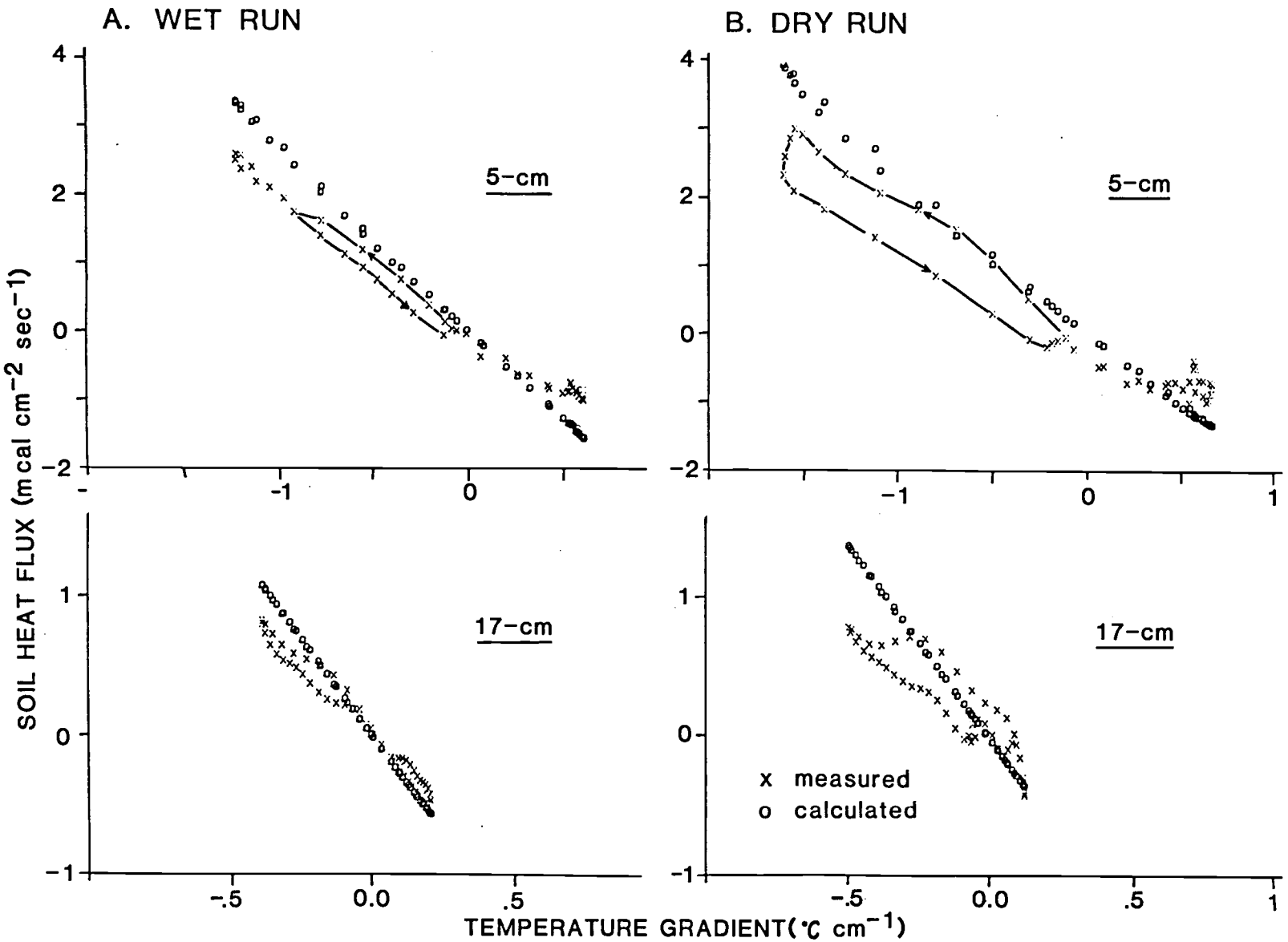

Figure 18. Relationship between the soil temperature gradient and calculated and measured soil heat flux at 5 and 17 cm on the wet (A) and dry (B) field plot.

For intermediate depths (5 and 17 cm) on the dry plot (Fig. 18b) a pronounced hysteresis loop in the measured soil heat flux during warming and cooling cycles exists. The loop indicates that the heat storage in these layers has not been fully accounted for by Equation [7] (Fuchs and Tanner, 1968). Inspection of Equation [7] indicates that dT/dt and the heat capacity of the soil, H, are two parameters that may contribute to erroneous estimates of heat storage. However negligible hysteresis exists in the measured fluxes (Fig. 18a) on the wet plot. Apparently stored heat was satisfactorily estimated in the wet but not the dry plot. Otherwise the experimental treatment of both plots was identical. Possibly water content changes as a consequence of field variability between the temperature probes and the location of soil water sampling were not always adequately assessed.

The nature of the hysteresis loop at 5 and 17 cm on the dry plot indicates that measured heat storage in these layers may have been overestimated. A reduction of storage in the warming limb of the measured heat flux for this portion of the profile will close the loop to resemble the wet plot. For those times of the day when dT/dt is large and heat capacity is overestimated the resulting error in heat flux will be greatest and vice versa (Equation [7] and [8]). At 1000 hours a 10% overestimation of heat capacity in the top 11 cm will result in a 7 and 6% overestimation of heat flux at 2 and 5 cm respectively.

The error introduced in the measured heat flux because heat storage was not fully accounted for is small compared to the differences between measured and calculated heat fluxes (Table 4). The outcome of this test is not considered to be a serious limitation to the conclusion of this study.

The regression for the calculated soil heat flux on the wet plot is strongly linear for most all depths. For the moisture and temperature regimes of the wet plot, a constant daily value of thermal conductivity (at a given depth), taken as the slope of the regression line, would have predicted soil heat flux equally as well as the 30-min. increments used in this paper. This same strong linearity is not apparent in the shallow depths of the dry soil. Extreme temperatures and gradients, as compared to the wet plot, coupled with larger isothermal latent heat fluxes may account for the curvilinear nature of these curves. A listing of the slopes of the curves shown in Figs. 18a and 18b is found in Table 5. The ratio of the measured heat flux slope to the calculated heat flux slope may be used as a general reduction factor for the de Vries thermal conductivity. Calculated thermal conductivity reduced by this factor will produce heat flux curves that resemble the measured values. This relationship gives no indication about the individual adjustments of conduction or vapor flux components of total heat flux.

An additional test of the calculated heat flux was made by isolating the vapor heat flux component from the total and comparing pure

Table 5. Slope of the linear regressions of heat flux and temperature gradient.

Depth	Null Alignment[1/]	Philip-de Vries[1/]	Null Alignment/ Philip-de Vries
	- - - - - - - - - - - - Wet treatment - - - - - - - - - - - -		
2	-1.522	-2.558	.595
5	-1.868	-2.650	.705
11	-1.768	-2.552	.693
17	-1.977	-2.754	.718
35	-1.708	-2.277	.750
	- - - - - - - - - - - - Dry treatment - - - - - - - - - - - -		
2	-1.128	-1.276	.884
5	-1.586	-2.266	.70
11	-1.612	-2.521	.639
17	-1.533	-2.772	.553
35	-1.842	-2.371	.777

[1/] The slope of the linear regression of heat flux and temperature gradient represents the soil thermal conductivity (mcal/cm·sec·C).

conduction heat flux with measured. These comparisons are shown in Figs. 19a and 19b for the wet and dry plots, respectively. A complete list of net daily soil heat flux by conduction is shown in Table 4. When the vapor component was eliminated heat flux by conduction still overestimated the measured seedzone heat flux by 20% in the dry plot. Predicted seedzone heat flux by conduction on the wet plot underestimated measured heat flux by 10%. Kimball et al. (1976) suggests that heat flux may be best estimated by ignoring vapor flux contributions and using pure conduction theory. These data support Kimball's observations. However they also provide evidence that vapor fluxes are actually underestimated and conduction fluxes are overestimated.

By assuming that liquid water fluxes were negligible in the dry plot observed water changes in soil slabs were compared directly to vapor flux predicted change. The net changes in water content, v_{i+1}^{i}, in a soil slab was calculated using a daily summation of the net vapor fluxes into and out of a soil slab for 30-min periods by:

$$v_{i+1}^{i} = \left[\sum_{n=1}^{48} \left(\left(\frac{Gv_{ij}+Gv_{i(j+1)}}{2\,L_{i(j+\frac{1}{2})}}\right) - \left(\frac{Gv_{(i+1)j}+Gv_{(i+1)(j+1)}}{2\,L_{(i+1)(j+\frac{1}{2})}}\right)\right)\right] \cdot \frac{60\ \text{sec}}{\text{min}} \cdot \frac{30\ \text{min}}{\text{period}} \quad \ldots\ (\text{cm/day}) \qquad [39]$$

Variables used in Equation [39] have been defined previously. The result of the summation will be a net vapor storage or loss in cm/day for a given soil layer. Results of this calculation are shown in Table 3. Calculated vapor flux on the dry plot underestimated the actual water content changes by a factor of two for most of the 3 to 11-cm profile. This very good agreement supports the Philip-de Vries

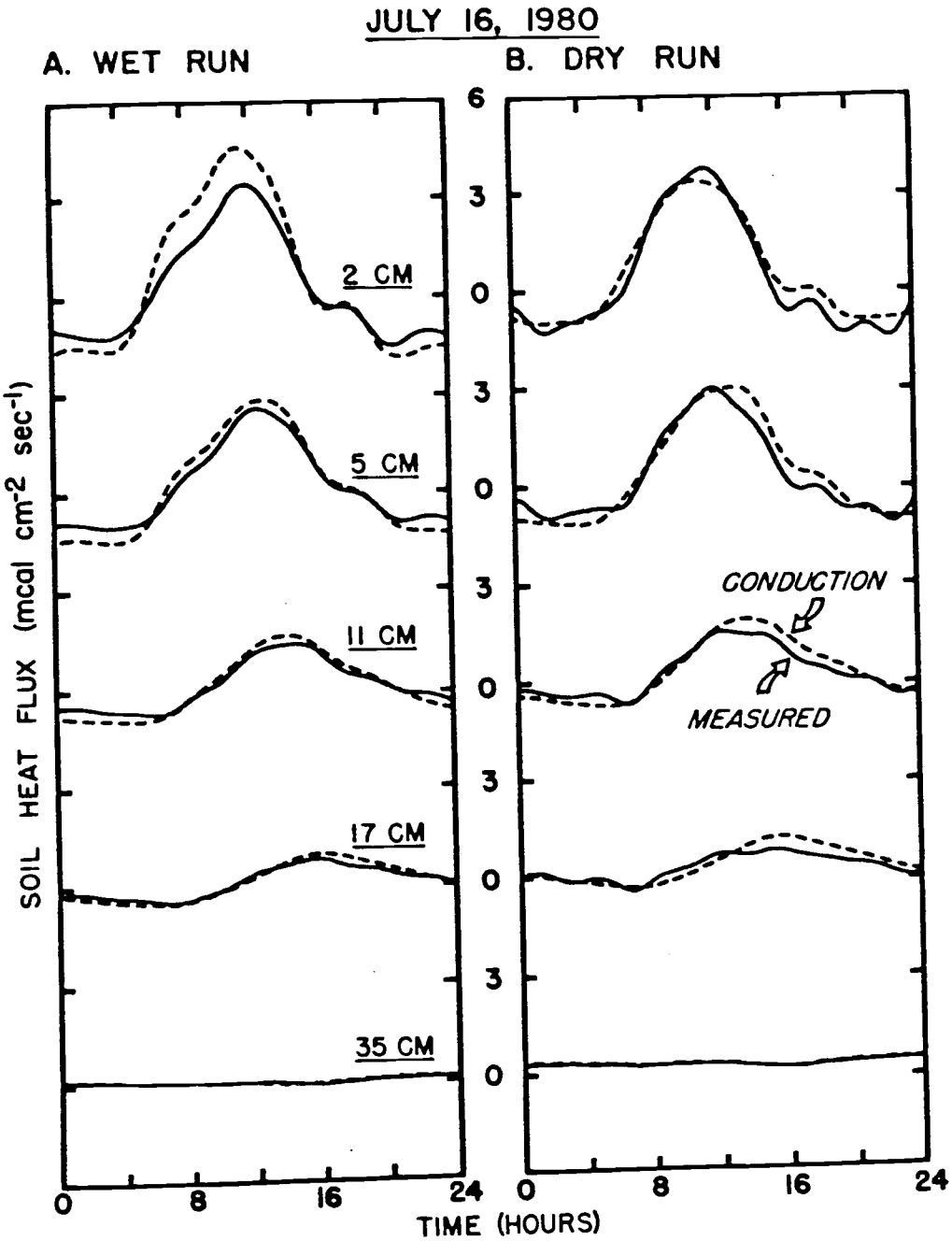

Figure 19. Diurnal measured and calculated conduction soil heat flux at 2, 5, 11, 17, and 35 cm on the wet (A) and dry (B) Walla Walla silt loam.

vapor prediction theory and suggests that the conduction component of the heat flux theory is overestimating soil heat flux. Thus, it does not seem a logical conclusion to ignore vapor flux to force an agreement of measured and Philip-de Vries heat flux.

That vapor flux is underestimated is consistent with the recent research findings of Jury and Letey (1979). They found that the phenomenological model of Cary (1963, 1964) describes thermal vapor fluxes if the phenomenological coefficient β has a value between 1.0 and 3.5, whereas the mechanistic theory of Philip and de Vries underpredicts vapor transport. Combined thermal and isothermal vapor fluxes for several times at 4 cm on the stubble plot were used to determine β for these data. Isothermal vapor flux contributed about 1% of the total calculated vapor flux at this depth. The comparisons consistently produced β values of 1.4 which is additional evidence that the de Vries estimated vapor fluxes are low.

At this point it is informative to briefly discuss some of the problems which are attendant with any field verification of model concepts. Field studies in heat and mass transfer are inherently difficult to conduct. These problems relate to soil variability and associated equipment costs to achieve precision. Based on qualitative procedural descriptions in earlier papers relating to replication or the number of sensory points experimental methods used here were considered adequate. During the analysis two shortcomings in the field methodology became apparent.

The soil thermocouple probes used to measure soil temperature did not accurately describe the thermal gradients in the top 2-cm of soil. A 5-mm diameter probe placed at a depth of 2.5-mm is integrating over

an increment of 2.5 to 7.5-mm. Near the surface where steep temperature gradients exist this will result in erroneous calculations of heat flux as evidenced by Table 4. Future field comparisons of this type must measure the soil temperature more accurately if advances are to be made in modeling coupled soil heat and water flow controlled by atmospheric variables. To this end a system is needed that uses small diameter soil probes for measurements near the surface coupled with an infrared surface temperature measurement.

Secondly, soil moisture changes may not have been accurately described in close proximity of the soil temperature sensors. By using a well collimated double probe radiation device measurements of soil water in centimeter slabs is possible. However this technology is costly and performance in the top 2 to 3-cm of soil is questionable. Further research is needed to evaluate the expected spatial variability of soil water in the horizon for various tillage practices. With a quantitative background to describe the spatial variation of water content (and temperature) the number and spacing of samples could be determined. Studies that evaluate the variability of field observations do exist (Wierenga et al., 1982). However, it appears that much of the information is site and tillage practice specific.

Conclusion

This field study provided a comparison of calculated total soil heat flux, by the methods of Philip-de Vries, with that measured by calorimetric accounting. Comparisons were made for both a wet and dry soil. Calculated fluxes included pure conduction and vapor heat fluxes.

For the dry soil conditions the vapor heat flux components were used to predict soil water changes. Calculated seedzone water content changes were compared to measured water changes.

At seedzone depths predicted daily heat fluxes were within 10% of the measured fluxes on the moist soil. For the dry conditions calculated fluxes overestimated measured flux by about 40%. Estimated heat flux by conduction alone improved the agreement between measured and calculated on the dry soil but underestimated fluxes on the moist soil. Seedzone water content changes in a dry soil, as predicted by heat flux in vapor movement, were underestimated by a factor of two. The general agreement between measured water changes and those changes predicted by vapor flux supports the mechanistic Philip-de Vries vapor flux theory even though vapor flux is underpredicted. However, because of a 10% overestimation of conduction fluxes even at 35 cm, on both plots, a further calibration of the de Vries thermal conductivity appears to be necessary for this soil.

The work reported here serves as a check of the Philip-de Vries predictive theory. Ultimately the evaluation of soil thermal properties will lead to the simulation of field moisture transport. The surface layer of soil couples the soil below to the atmosphere above. Meteorological conditions determine evaporation when the surface layer is wet, but when the soil dries the transport properties of the surface slab will limit evaporation rates. This validation work coupled with existing evaporative models, most notably that of Hammel (1979), could provide the basis for a rigorous treatment of tillage effects on soil moisture conservation.

BIBLIOGRAPHY

Allmaras, R. R., E. A. Hallauer, W. W. Nelson, and S. D. Evans. 1977. Surface energy balance and soil thermal property modifications by tillage-induced soil structure. Minnesota Agr. Exp. Sta. Tech. Bul. 306. 40 pp.

Allmaras, R. R., K. Ward, C. L. Douglas Jr., L. G. Ekin. 1982. Long-term cultivation effects on hydraulic properties of a Walla Walla silt loam. Soil and Tillage Research, 2 (1982) 265-279.

Bouwer, H. 1962. Field determination of hydraulic conductivity above a water table with the double-tube method. Soil Sci. Soc. Amer. Proc. 26:330-335.

Boynton, W. P., and Brattain, W. H. 1929. Interdiffusion of gases and vapors. International Critical Tables, Vol. 5, pp. 62-63, McGraw-Hill Book Co., New York.

Campbell, G. S. 1977. An introduction to environmental biophysics. Springer-Verlag, Inc., New York. 159 p.

Cary, J. W. 1963. Onsager's relation and the non-isothermal diffusion of water vapor. J. Phys. Chem. 67:126-129.

Cary, J. W. 1964. An evaporation experiment and its irreversible thermodynamics. Int. J. Heat Mass Transfer 7:531-538.

Cary, J. W. 1966. Soil moisture transport due to thermal gradients: Practical aspects. Soil Sci. Soc. Am. Proc., 30:428-433.

Choudhary, M. A., and C. J. Baker. 1981. Physical effects of direct drilling equipment on undisturbed soils. III. wheat seedling performance and in-groove micro-environment in a dry soil. N.Z. J. Ag. Res. 24:189-195.

Cochran, P. H., L. Boersma, and C. T. Youngberg. 1967. Thermal properties of a pumice soil. Soil Sci. Soc. Amer. Proc. 31:454-459.

Cochran, V. L., R. I. Papendick, and C. D. Fanning. 1970. Early fall crop establishment to reduce winter runoff and erosion on Palouse slopes. J. Soil Water Conserv. 25:231-234.

Collis-George, N., and M. O. Melville. 1978. Water absorption by swelling seeds. II. Surface condensation boundary condition. Aust. J. Soil Res. 16:291-310.

Currie, J. A. 1960. Gaseous diffusion in porous media. II. Dry granular materials. Br. J. Appl. Phys. 11:318.

Currie, J. A. 1961. Gaseous diffusion in porous media. III. Wet granular materials. Br. J. Appl. Phys. 12:275.

de Vries, D. A. 1958. Simultaneous transfer of heat and moisture in porous media. Trans. Am. Geophys. Union 39:909-916.

de Vries, D. A. 1963. Thermal properties of soils. In: W. R. van Wijk (Editor). Physics of Plant Environment. North-Holland, Amsterdam, pp 210-235.

de Vries, D. A. 1975. Heat transfer in soils. In: D. A. de Vries and N. H. Afgan (Editors). Heat and mass transfer in the biosphere. John Wiley and Sons, pp. 5-28.

Dorsey, N. E. 1940. Properties of ordinary water-substance. Reinhold Publishing Corp., New York. 673 p.

Farrell, D. A., E. L. Greacen, and C. G. Gurr. 1966. Vapor transfer in soil due to air turbulence. Soil Sci. 102:305-313.

Fink, D. H. and R. D. Jackson. 1973. An equation for describing water vapor adsorption isotherms of soils. Soil Sci. 116:256-261.

Fuchs, M. and C. B. Tanner. 1968. Calibration and field test of soil heat flux plates. Soil Sci. Soc. Am. Proc. 32, 326-328.

George, G. O. 1982. Best management practices and water quality demonstration and evaluation project. Spec. Rept. 646. Oregon Agric. Expt. Sta., Corvallis, OR.

Goff, J. A., and Gratch, S. 1946. Trans. Amer. Soc. Heat. and Vent. Eng., Vol. 52, p. 95.

Greb, B. W. 1966. Effect of surface-applied wheat straw on soil water losses by solar distillation. Soil Sci. Soc. Am. Proc. 30:786-788.

Green, R. E. and J. C. Corey. 1971. Calculation of hydraulic conductivity: A further evaluation of some predictive methods. Soil Sci. Soc. Am. Proc. 35:3-8.

Hadas, A. 1977. Evaluation of theoretically predicted thermal conductivities of soils under field and laboratory conditions. Soil Sci. Soc. Am. J. 41:460-466.

Hammel, J. E. 1979. Modeling tillage effects on evaporation and seed-zone water content during fallow in eastern Washington. Ph.D. Thesis, Washington State University, Pullman, Washington.

Hanks, R. J. and N. P. Woodruff. 1958. Influence of wind and water vapor transfer through soil, gravel and straw mulches. Soil Sci. 86:160-164.

Jackson, R. D. 1965. Water vapor diffusivity in relatively dry soil: IV. Temperature and pressure effects on sorption diffusion coefficients. Soil Sci. Soc. Am. Proc. 29:144-148.

Jackson, R. D. 1973. Diurnal changes in soil water content during drying. p. 37-55. In R. R. Bruce et al. (ed.) Field Soil Water Regime. Spec. Publ. 5., Soil Sci. Soc. Am.

Jackson, R. D., B. A. Kimball, R. J. Reginato, S. B. Idso, and F. S. Nakayama. 1975. Heat and water transfer in a natural soil environment. In D. A. de Vries and H. H. Afgan (eds.), Heat and mass transfer in the biosphere. Part 1. Transfer processes in the plant environment. Scripta, Washington, D.C. pp. 67-76.

Jury, W. A. 1973. Simultaneous transport of heat and moisture through a medium sand. Ph.D. Thesis, University of Wisconsin, Madison.

Jury, W. A. and J. Letey Jr. 1979. Water vapor movement in soil: Reconciliation of theory and experiment. Soil Sci. Soc. Am. J. 43:823-827.

Kimball, B. A., and E. R. Lemon. 1971. Air turbulent effects upon soil gas exchange. Soil Sci. Soc. Am. Proc. 35:16-20.

Kimball, B. A. and R. D. Jackson. 1975. Soil-heat flux determination: A null-alignment method. Agric. Meteorol. 15:1-9.

Kimball, B. A. 1975. Cubic Spline Smoothing, U.S. Water Conservation Laboratory, WCL Report 9, USDA-ARS, Phoenix, Arizona.

Kimball, B. A. 1976. Smoothing data with cubic splines. Agron. J. 68:126-129.

Kimball, B. A., R. D. Jackson, R. J. Reginato, F. S. Nakayama, and S. B. Idso. 1976. Comparison of field-measured and calculated soil-heat fluxes. Soil Sci. Soc. Amer. J. 40:18-25.

Krischer, O., and H. Rohnalter. 1940. Warmeleitung and dampfdiffusion in feuchten gutern. U.P.I. Forschungsheft 402.

Leggett, G. E., R. E. Ramig, L. C. Johnson, and T. W. Massee. 1974. Summer fallow in the Pacific Northwest. Conserv. Res. Report No. 17. Agricultural Research Service, USDA.

Lindstrom, M. J., R. I. Papendick and F. E. Koehler. 1976. A model to predict winter wheat emergence as affected by soil temperature, water potential, and depth of planting. Agron. J. 68:137-140.

List, R. J. 1958. Smithsonian meteorological tables. Smithsonian Institution, Washington. 527 p.

Myrold, D. D., L. F. Elliott, R. I. Papendick, and G. S. Campbell. 1981. Water potential - water content characteristics of wheat straw. Soil Sci. Soc. Am. J. 45:329-333.

Oke, T. R. 1978. Boundary layer climates. University Paperbacks, Methuen and Co. Ltd., London. 372 p.

Panofsky, H. A. and G. W. Brier. 1968. Some applications of statistics to meteorology, The Pennsylvania State University, University Park, Penn. 224 pp.

Papendick, R. I., M. J. Lindstrom, and V. L. Cochran. 1973. Soil mulch effects on seedbed temperature and water during fallow in eastern Washington. Soil Sci. Soc. Amer. Proc. 37:307-314.

Philip, J. R. 1957. Evaporation, and moisture and heat fields in the soil. J. Meteorol. 14:354-366.

Philip, J. R. and D. A. de Vries. 1957. Moisture movement in porous materials under temperature gradients. Trans. Am. Geophys. Union. 38:222-232.

Pikul, J. L. Jr., R. R. Allmaras, and G. E. Fischbacher. 1979. Incremental soil sampler for use in summer-fallowed soils. Soil Sci. Soc. Amer. J. 43:425-427.

Pikul, J. L. Jr. 1982. Formation of soil frost as influenced by crop residue management. In 1982 Research Report, Columbia Basin Agricultural Res., Spec. Rpt. 661. Oregon Agric. Expt. Sta., Corvallis, Or.

Rogers, R. B., S. Dubetz. 1979. Effect of soil-seed contact on seed imbibition. Can. Agric. Eng. 22:89-92.

Scotter, D. R., G. W. Thurtell, and P. A. Raats. 1967. Dispersion resulting from sinusoidal gas flow in porous media. Soil Sci. 104: 306-308.

Sepaskhah, A. R. 1974. Experimental analysis of subsurface heating and irrigation on the temperature and water content of soils. Ph.D. Thesis Oregon State University, Corvallis, Or.

Sepaskhah, A. R. and L. Boersma. 1979. Thermal conductivity of soils as a function of temperature and water content. Soil Sci. Soc. Am. Proc. 43:439-444.

Swokowski, E. W. 1978. Calculus With Analytic Geometry. Prindle, Weber and Schmidt; Boston, Mass. pp 578-582.

Tanner, C. B. 1963. Basic instrumentation and measurements for plant environment and micrometeorology. Soils Bull. 6. Univ. of Wis., Madison.

VanBavel, C. H. M. 1952. Gaseous diffusion and porosity in porous media. Soil Sci. 73:91-104.

VanWijk, W. R., W. E. Larson, and W. C. Burrows. 1959. Soil temperature and the early growth of corn from mulched and unmulched soil. Soil Sci. Soc. Am. Proc. 23:428-434.

Wierenga, P. J., D. R. Nielsen, and R. M. Hagen. 1969. Thermal properties of a soil based upon field and laboratory measurements. Soil Sci. Soc. Am. Proc. 33:354-360.

Wierenga, P. J., D. R. Nielsen, R. Horton, B. Kies. 1982. Tillage effects on soil temperature and thermal conductivity. In D. M. Van Doren (ed. chm.) Predicting tillage effects on soil physical properties and processes. ASA Spec. Publ. 44.

Wilkins, D. E., R. R. Allmaras, G. A. Muilenberg, C. E. Johnson. 1981. Effect of grain drill opener on wheat emergence. Am. Soc. Ag. Eng. Paper No. 81-1021. American Society of Agricultural Engineers, P. O. Box 410, St. Joseph, MO 49085.

APPENDICES

Appendix 1. Methodology used to obtain dH/dz in Equation [4].

This section is included to illustrate the method used to obtain dH/dz in Equation [4]. In the material and methods section, determination of $d\theta/dz$, at the depths and times corresponding to soil temperature measurements, has been discussed. Knowing $d\theta/dz$ and the relationship of soil water potential, Ψ, to θ allowed a determination of dH/dz at the depths and times corresponding to soil temperature measurements.

The smoothed water release curve (Fig. 5a) is defined by a 3rd degree polynomial having the general form:

$$\ln\Psi = a_0+a_1\theta+a_2\theta^2+a_3\theta^3 \ldots\ldots \text{(bar)}$$

where the above coefficients are defined in Appendix 3.

Hydraulic head, H, is defined as:

$$H = -1000 \exp[a_0+a_1\theta+a_2\theta^2+a_3\theta^3]-Z \ldots\ldots \text{(cm)}$$

from which the derivative with respect to θ, $dH/d\theta$, is:

$$dH/d\theta = -1000 \exp[a_0+a\theta_1+a_2\theta^2+a_3\theta^3]\cdot[a_1+2a_2\theta+3a_3\theta^2] \ldots\ldots \text{(cm)}$$

To obtain $(dH/dz)_{ij}$, cm/cm, the above equation is evaluated at the desired θ_{ij}. Both the left and right hand sides are multiplied by $(d\theta/dz)_{ij}$. On the left hand side $d\theta$ cancels yielding dH/dz.

Appendix 2. Analysis of the error introduced in the apparent soil thermal conductivity by incorrectly evaluating the diffusivity of water vapor in air.

This section is presented as an example calculation of vapor conductivity using the published methodology as found in de Vries (1963 and 1976) and Kimball et al. (1976). Although all calculations generally follow Philip and de Vries (1957), strict adherence to the methods of de Vries (1963) will produce serious error when compared to the methods of de Vries (1976) and Kimball et al. (1976). The examples use the following soil conditions and constants:

Temperature (T) = 20°C (293 K)

Total pressure of soil atmosphere (P) = 1 bar (750 mm Hg)

Relative humidity of soil atmosphere (h) = 0.98

Gas constant (R) = 83138 mbar·cm^3/mol K (1987.2 mcal/mol·K)

Gas constant for water vapor (Rw) = 110.2985 mcal/g·K

Saturated vapor pressure over water (Pw^S) as a function of temperature are available from tables (List, 1958) or the Goff-Gratch (1946) formulation. For this example a simplified approximation will be used (Campbell, 1977).

$$Pw^S = 10 \exp \left(52.57633 - \frac{6790.4985}{°K} - 5.02808 \ln °K\right)$$

where Pw^S is in mbar and K is Kelvin temperature. From which

$$\frac{dPw^S}{dK} = Pw \left(\frac{6790.4985}{K^2} - \frac{5.028008}{K}\right)$$

and for the given conditions

$$Pw^S = 23.1684 \text{ mbar } (17.3763 \text{ mm Hg})$$

$$\frac{dPw^S}{dK} = 1.4350 \text{ mbar/K } (1.0762 \text{ mm Hg/K})$$

Latent heat of vaporization of water, L, is calculated using Equation [16] for 20°C

$$L = 584940 \text{ mcal/g}$$

de Vries (1963)

The vapor conductivity (λv) when the soil air is not saturated with water vapor is written following de Vries (1963) as:

$$\lambda v = \frac{h\ L\ Da\ P}{Rw\ K\ (P-Pw^S)} \frac{dPw^S}{dK}$$

where the diffusion coefficient for water vapor in air, determined by Krischer and Rohnalter (1940), is represented in the range 20° to 70°C by the expression

$$Da = \frac{17.6}{P} \left(\frac{K}{273}\right)^{2.3}$$

where Da is expressed in cm^2/sec and P in mm Hg. For the given conditions

$$Da = 0.0276 \text{ } cm^2/sec$$

and

$$\lambda v = 0.5394 \text{ mbar} \cdot cm^2/sec \cdot K; (1 \text{ mbar} = 0.0239 \text{ mcal}/cm^3)$$

$$\lambda v = 0.0129 \text{ mcal/cm} \cdot \text{sec} \cdot K$$

de Vries (1976)

As written by de Vries (1976) the apparent contribution to the thermal conductivity of air due to vapor diffusion is given by:

$$\lambda v = \frac{h\ L\ Da\ M\ P}{R\ K\ (P - Pw^S)} \left(\frac{dPw^S}{dK}\right)$$

where M is the molar mass of water (18.016 g/mol) and the diffusion coefficient of water vapor in air can be found as (Boynton and Brattain, 1929)

$$Da = C\ (Po/P)(K/Ko)^{n} \cdot (cm^2/100\ mm^2)$$

with Po = 1 atm = 760 mm Hg, Ko = 273.15 K, C = 21.7 mm^2/s, n = 1.88

from which Da = .2509 cm^2/sec

and

$$\lambda v = 4.9030\ mbar \cdot cm^2/sec \cdot K\ (0.1172\ mcal/cm \cdot sec \cdot K)$$

Kimball et al. (1976)

The methodology of Kimball et al. (1976) has been adopted for this work and vapor conductivity is written as:

$$\lambda v = h\ L\ Da\gamma\ (d\rho o/dT)$$

where the above variables are defined using Equation [14] through [23] from which

$Da = 0.2592\ cm^2/sec$

$\gamma = 1.0231$

$(d\rho o/dT) = 9.9 \times 10^{-7}\ g/cm^3 \cdot C$

$\lambda v = 0.1503\ mcal/cm \cdot sec \cdot K$

From the above example the most notable discrepancy between all the formulations is the value of Da obtained by the methods of de Vries (1963). As a comparison the value from List (1958) is 0.257 cm^2/sec. The error in evaluating Da by the formulation in de Vries (1963) would underestimate λv by a factor of ten as compared to the other examples.

Apparent soil thermal conductivity, with λv = 0.1503, using Equation [11] and the following:

Xw = 0.25	λw = 1.4213 mcal/cm•sec•C	
Xa = 0.29	λa = 0.0597	Ka = 1.6106 (ga = 0.143)
Xs = 0.46	λs = 9.98	Ks = 0.4201 (gs = 0.144)
	λv = 0.1503	
	λav= 0.21	

would be 2.6162 mcal/cm•sec•C

However, if an error was made in calculating Da and the resulting λv was a factor of ten low, then the apparent soil thermal conductivity, with λv = 0.01503, using Equation [11] and the following:

Xw = 0.25	λw = 1.4213		
Xa = 0.29	λa = 0.0597	Ka =	Ka = 1.8015 (ga = 0.143)
Xs = 0.49	λs = 9.98		Ks = 0.4201 (gs = 0.144)
	λv = 0.01503		
	λav= 0.0747		

would be 2.4055 mcal/cm•sec•C or a 10% underestimation of the soil thermal conductivity and heat flux.

Appendix 3. Equations describing the smoothed curves of Figs. 3, 5a, 5b, 6, 13, and 14.

Smoothed curves are defined by 3rd degree polynomials having the general form $y = a_0+a_1x+a_2x^2+a_3x^3$.

Fig. 3 - Soil Bulk Density

Z	a_0	a_1	a_2	a_3
0.25-5.0	1.019958	0.166618	-0.039014	0.002792
5-17	1.383695	-0.051624	0.004634	-0.000117
17-30	0.584736	0.089368	-0.003659	0.000045
30-35	1.939694	-0.046127	0.000856	-0.000005

Fig. 5a - Log_e Water Potential (bar)

θ	a_0	a_1	a_2	a_3
0.10-0.22	7.83613	-47.9265	-40.7657	352.0841
0.22-0.27	36.6396	-440.7018	1744.5762	-2352.9795
0.27-0.32	-46.2432	480.2188	-1666.2410	1857.9060
0.32-0.39	15.0304	-94.2216	128.8854	-12.0174

Fig. 5b - Log_e Hydraulic Conductivity (cm/min)

θ	a_0	a_1	a_2	a_3
0.10-0.40	-40.2686	227.3224	-592.8967	592.2188

Fig. 6 - Soil Organic Fraction

Z	a_0	a_1	a_2	a_3
0.25-15	0.0201451	-0.0000638	0.0000132	-0.0000005
15-20	0.0310378	-0.0022423	0.0001584	-0.0000037
20-25	-0.0509559	0.0100567	-0.0004564	0.0000064
25-55	0.0575897	-0.0029687	0.0000645	-0.0000004

Fig. 13 - Ds/Do

ε	a_0	a_1	a_2	a_3
0.0-1.0	-0.000130	0.646193	-0.788531	1.142125

Fig. 14 - D/Ds

$\varepsilon g/\varepsilon$	a_0	a_1	a_2	a_3
0.0-0.4	0.000401	0.229197	0.617195	-0.210589
0.4-0.55	-1.897447	14.463061	-34.967465	29.443294
0.55-0.65	17.455299	-91.097376	156.960603	-86.876747
0.65-1.0	-11.743369	43.665712	-50.367226	19.445216